

Phenomenological aspects of a fermiophobic $SU(2) \times SU(2) \times U(1)$ extension of the Standard Model

Andrea Donini¹

Dipartimento di Fisica, Università ‘La Sapienza’, I-00185 Rome, Italy

Ferruccio Feruglio², Joaquim Matias³

Dipartimento di Fisica, Università di Padova, I-35131 Padua, Italy

and

Fabio Zwirner⁴

INFN, Sezione di Padova, I-35131 Padua, Italy

Abstract

We consider an extension of the standard electroweak theory with gauge group $SU(2)_L \times SU(2)_R \times U(1)_{\tilde{Y}}$, where the gauge bosons of the extra $SU(2)_R$ factor do not couple to ordinary fermions. We show that precision electroweak data and flavour physics provide quite stringent indirect constraints on its parameter space, but still allow for relatively light non-standard gauge and Higgs bosons. We then consider the model phenomenology at high-energy colliders, and observe that in the gauge boson sector present bounds and possible future signals are dominated by Z' production. In summary, indirect constraints on the charged gauge boson sector are so tight that observable new effects must be connected either with the neutral gauge boson sector or with the extended Higgs sector of the model.

May 1997

¹e-mail address: donini@vxrm70.roma1.infn.it

²e-mail address: feruglio@padova.infn.it

³e-mail address: matias@padova.infn.it

⁴e-mail address: zwirner@padova.infn.it

1 Introduction

Extensions of the Standard Model (SM) of electroweak interactions based on the gauge group $SU(2)_L \times SU(2)_R \times U(1)_{\tilde{Y}}$ (for the time being, the labelling of the different factors is purely conventional) have been widely discussed in the literature [1–5], with various motivations. In particular, these models are a natural framework to parametrize the possible existence of additional W' and Z' bosons, detectable at present and future colliders.

To limit the number of possibilities, we restrict our attention to models with the following properties: (i) they are non-supersymmetric; (ii) their fermionic sector consists only of $SU(2)$ singlets and doublets; (iii) their Higgs sector consists only of $SU(2)$ singlets, doublets and triplets; (iv) they admit the standard embedding of the electric charge:

$$Q = T_{3L} + T_{3R} + \tilde{Y} ; \quad (1.1)$$

(v) the gauge interactions are universal for the three fermion generations. Even under the above assumptions, a considerable freedom remains, which allows for at least five different models¹:

- the ‘standard’ [1] left-right symmetric model (LR);
- the ‘leptophobic’ model (LP);
- the ‘hadrophobic’ model (HP);
- the ‘fermiophobic’ [3] model (FP);
- the ‘ununified’ [4] model (UN).

The various models are defined by the transformation properties of their fermion content with respect to the gauge group, summarized in table 1. Notice that some of the models (LR, HP) include right-handed neutrinos ν_R , whilst some others (LP, FP, UN) have exactly the fermion content of the SM. The Higgs fields that can play a role in the spontaneous breaking of the gauge symmetry, assumed to proceed according to the following pattern

$$SU(2)_L \times SU(2)_R \times U(1) \longrightarrow U(1)_{e.m.} , \quad (1.2)$$

are those transforming non-trivially under the gauge group but containing at least one electrically neutral component, and are listed in table 2. Those needed to get an acceptable tree-level fermion mass spectrum are marked with the symbol \otimes . Others, as we shall see, may be needed to get an acceptable mass spectrum in the gauge boson sector: standard choices are marked with the symbol \times .

¹Of course, further models can be constructed by relaxing one or more of the previous assumptions: an example is the ‘topflavor’ model [5], where $SU(2)_L$ acts on the first two generations and $SU(2)_R$ on the third one.

<i>Field/Model</i>	<i>LR</i>	<i>LP</i>	<i>HP</i>	<i>FP</i>	<i>UN</i>
$q_L \equiv \begin{pmatrix} u_L \\ d_L \end{pmatrix}$	(2, 1, 1/6)	(2, 1, 1/6)	(2, 1, 1/6)	(2, 1, 1/6)	(2, 1, 1/6)
$q_R \equiv \begin{pmatrix} u_R \\ d_R \end{pmatrix}$	(1, 2, 1/6)	(1, 2, 1/6)	$\begin{pmatrix} (1, 1, 2/3) \\ (1, 1, -1/3) \end{pmatrix}$	$\begin{pmatrix} (1, 1, 2/3) \\ (1, 1, -1/3) \end{pmatrix}$	$\begin{pmatrix} (1, 1, 2/3) \\ (1, 1, -1/3) \end{pmatrix}$
$l_L \equiv \begin{pmatrix} \nu_L \\ e_L \end{pmatrix}$	(2, 1, -1/2)	(2, 1, -1/2)	(2, 1, -1/2)	(2, 1, -1/2)	(1, 2, -1/2)
$l_R \equiv \begin{pmatrix} \nu_R \\ e_R \end{pmatrix}$	(1, 2, -1/2)	$\begin{matrix} - \\ (1, 1, -1) \end{matrix}$	(1, 2, -1/2)	$\begin{matrix} - \\ (1, 1, -1) \end{matrix}$	$\begin{matrix} - \\ (1, 1, -1) \end{matrix}$

Table 1: *Fermion transformation properties in the models considered in the text. The numbers in brackets refer to $SU(2)_L$, $SU(2)_R$ and $U(1)_{\tilde{Y}}$, respectively. Colour and generation indices are implicit.*

In the class of models considered above, we would like to select a candidate model that can naturally satisfy all the existing phenomenological constraints and, at the same time, allow for relatively light extra gauge bosons, accessible to future accelerators such as the upgraded Tevatron collider and the LHC. In our opinion, a palatable candidate is the FP model: it is automatically free of gauge anomalies (in contrast with the LP, HP and UN models); it does not contain right-handed neutrinos, so it can do without Higgs triplets and still provide an acceptable tree-level fermion and gauge boson mass spectrum (in contrast with the LR and HP models); it automatically guarantees the absence of flavour-changing neutral currents (FCNC) at tree level, and the suppression of loop-induced effects, thanks to the fact that the unmixed $SU(2)_R$ gauge bosons and the (ϕ_{LR}, ϕ_R) Higgs bosons cannot have gauge-invariant couplings to the matter fermions (in contrast with all the other models of our list).

For the above reasons, in the rest of this paper we restrict our attention to the FP model, and present a phenomenological analysis of it as complete as possible. In section 2 we discuss the general structure of the FP model, considering first masses and mixings in

<i>Field/Model</i>	<i>LR</i>	<i>LP</i>	<i>HP</i>	<i>FP</i>	<i>UN</i>
$\phi_{LR} \equiv \begin{pmatrix} \phi_1^0 & \phi_2^+ \\ \phi_1^- & \phi_2^0 \end{pmatrix} \sim (2, 2, 0)$	\otimes	\otimes	\otimes	\times	\times
$\phi_L \equiv \begin{pmatrix} \phi_L^0 \\ \phi_L^- \end{pmatrix} \sim (2, 1, -1/2)$	$-$	\otimes	\otimes	\otimes	\otimes
$\phi_R \equiv \begin{pmatrix} \phi_R^0 \\ \phi_R^- \end{pmatrix} \sim (1, 2, -1/2)$	$-$	$-$	$-$	\times	\otimes
$\Delta_L \equiv \begin{pmatrix} \frac{1}{\sqrt{2}}\delta_L^+ & \delta_L^{++} \\ \delta_L^0 & -\frac{1}{\sqrt{2}}\delta_L^+ \end{pmatrix} \sim (3, 1, 1)$	\times	$-$	$-$	$-$	$-$
$\Delta_R \equiv \begin{pmatrix} \frac{1}{\sqrt{2}}\delta_R^+ & \delta_R^{++} \\ \delta_R^0 & -\frac{1}{\sqrt{2}}\delta_R^+ \end{pmatrix} \sim (1, 3, 1)$	\otimes	$-$	\otimes	$-$	$-$

Table 2: *Typical sets of Higgs fields for the models considered in the text.*

the various sectors, and then gauge and Yukawa interactions in the mass eigenstate basis. Section 3 deals with the many facets of the FP-model phenomenology: constraints from precision electroweak data and from flavour physics, as well as production and decay of W' and Z' bosons at hadron colliders. Some useful formulae are collected in the appendices.

2 General structure of the fermiophobic model

The FP model is described by a gauge-invariant Lagrangian density of the form

$$\mathcal{L} = \mathcal{L}_{YM} + \mathcal{L}_S + \mathcal{L}_F + \mathcal{L}_Y. \quad (2.1)$$

The Yang-Mills term \mathcal{L}_{YM} is given by:

$$\mathcal{L}_{YM} = -\frac{1}{4}F_{L\mu\nu}^a F_L^{a\mu\nu} - \frac{1}{4}F_{R\mu\nu}^a F_R^{a\mu\nu} - \frac{1}{4}B_{\mu\nu}B^{\mu\nu} + \dots, \quad (2.2)$$

where the dots stand for terms involving the gluons and

$$\begin{aligned}
F_{L\mu\nu}^a &= \partial_\mu W_{L\nu}^a - \partial_\nu W_{L\mu}^a + g_L \epsilon^{abc} W_{L\mu}^b W_{L\nu}^c, \\
F_{R\mu\nu}^a &= \partial_\mu W_{R\nu}^a - \partial_\nu W_{R\mu}^a + g_R \epsilon^{abc} W_{R\mu}^b W_{R\nu}^c, \\
B_{\mu\nu} &= \partial_\mu B_\nu - \partial_\nu B_\mu.
\end{aligned} \tag{2.3}$$

The term \mathcal{L}_S , containing generalized kinetic terms and self-interactions of the spin-0 fields, is given by:

$$\mathcal{L}_S = (D^\mu \phi_L)^\dagger D_\mu \phi_L + (D^\mu \phi_R)^\dagger D_\mu \phi_R + \text{tr} \left[(D^\mu \phi_{LR})^\dagger D_\mu \phi_{LR} \right] - V_0, \tag{2.4}$$

where V_0 is the scalar potential, a gauge-invariant polynomial of degree four in the fields $(\phi_L, \phi_R, \phi_{LR})$ and their hermitean conjugates, and the covariant derivatives read:

$$\begin{aligned}
D_\mu \phi_L &= (\partial_\mu - ig_L W_{L\mu}^a \frac{\tau^a}{2} + \frac{i}{2} \tilde{g} B_\mu) \phi_L, \\
D_\mu \phi_R &= (\partial_\mu - ig_R W_{R\mu}^a \frac{\tau^a}{2} + \frac{i}{2} \tilde{g} B_\mu) \phi_R, \\
D_\mu \phi_{LR} &= \partial_\mu \phi_{LR} - ig_L W_{L\mu}^a \frac{\tau^a}{2} \phi_{LR} + ig_R W_{R\mu}^a \phi_{LR} \frac{\tau^a}{2}.
\end{aligned} \tag{2.5}$$

The term \mathcal{L}_F contains the fermion kinetic terms and gauge interactions: since in the FP model all fermions are $SU(2)_R$ singlets, their gauge interactions are exactly the same as in the SM, when expressed in terms of the gauge vector bosons $(W_{L\mu}^a, B_\mu)$ and of the corresponding coupling constants (g_L, \tilde{g}) . Finally, the term \mathcal{L}_Y describes the Yukawa interactions. In the FP model, the only couplings allowed by gauge invariance are those between the fermions and the $SU(2)_L$ doublet ϕ_L , thus \mathcal{L}_Y coincides with its SM counterpart. In terms of the quark and lepton mass eigenstates, represented by three-dimensional vectors in flavour space:

$$\begin{aligned}
\mathcal{L}_Y &= -\frac{\sqrt{2}}{v_L} \left[(\overline{u}_L M_{diag}^U u_R + \overline{d}_L M_{diag}^D d_L + \overline{e}_L M_{diag}^E e_L) \phi_L^0 \right. \\
&\quad \left. + (\overline{d}_L K^\dagger M_{diag}^U u_R - \overline{d}_L M_{diag}^D K^\dagger u_L - \overline{e}_L M_{diag}^E \nu_L) \phi_L^- + \text{h.c.} \right],
\end{aligned} \tag{2.6}$$

where $M_{diag}^U = (m_u, m_c, m_t)$, $M_{diag}^D = (m_d, m_s, m_b)$, $M_{diag}^E = (m_e, m_\mu, m_\tau)$, and K is the Cabibbo-Kobayashi-Maskawa matrix.

2.1 Mass spectrum

To discuss the spectrum of the model, we assume that an appropriate choice of parameters in the scalar potential V_0 leads to the following pattern of vacuum expectation values (VEVs) for the scalar fields:

$$\langle \phi_{LR} \rangle = \frac{1}{\sqrt{2}} \begin{pmatrix} v_1 & 0 \\ 0 & v_2 \end{pmatrix}, \quad \langle \phi_L \rangle = \frac{1}{\sqrt{2}} \begin{pmatrix} v_L \\ 0 \end{pmatrix}, \quad \langle \phi_R \rangle = \frac{1}{\sqrt{2}} \begin{pmatrix} v_R \\ 0 \end{pmatrix}. \tag{2.7}$$

We also assume that (v_L, v_R, v_1, v_2) are real, and define the auxiliary quantities:

$$u^2 \equiv v_1^2 + v_2^2, \quad \tan \beta \equiv \frac{v_2}{v_1}, \quad g \equiv g_L, \quad x \equiv \frac{g_R}{g}, \quad y \equiv \frac{\tilde{g}}{g}. \quad (2.8)$$

Before specializing to the charged and neutral gauge bosons, it is convenient to recall the general solution of the eigenvalue problem for a 2×2 mass matrix, in a way suitable for taking the physically interesting limit of small mixing. In the interaction basis, $(V_1, V_2) \equiv (V_{SM}, V_{extra})$:

$$\mathcal{M}^2 = \begin{pmatrix} \mathcal{M}_{11} & \mathcal{M}_{12} \\ \mathcal{M}_{12} & \mathcal{M}_{22} \end{pmatrix}. \quad (2.9)$$

In our conventions, we denote mass eigenvalues and eigenstates by:

$$m_V^2 = \frac{1}{2} \left[\mathcal{M}_{11} + \mathcal{M}_{22} - \sqrt{(\mathcal{M}_{11} - \mathcal{M}_{22})^2 + 4\mathcal{M}_{12}^2} \right], \quad (2.10)$$

$$m_{V'}^2 = \frac{1}{2} \left[\mathcal{M}_{11} + \mathcal{M}_{22} + \sqrt{(\mathcal{M}_{11} - \mathcal{M}_{22})^2 + 4\mathcal{M}_{12}^2} \right], \quad (2.11)$$

$$\begin{pmatrix} V \\ V' \end{pmatrix} = \begin{pmatrix} c_\alpha & s_\alpha \\ -s_\alpha & c_\alpha \end{pmatrix} \begin{pmatrix} V_1 \\ V_2 \end{pmatrix}, \quad (2.12)$$

where $c_\alpha \equiv \cos \alpha$ and $s_\alpha \equiv \sin \alpha$, with

$$\sin 2\alpha = \frac{-2\mathcal{M}_{12}}{\sqrt{(\mathcal{M}_{11} - \mathcal{M}_{22})^2 + 4\mathcal{M}_{12}^2}}, \quad \cos 2\alpha = \frac{\mathcal{M}_{22} - \mathcal{M}_{11}}{\sqrt{(\mathcal{M}_{11} - \mathcal{M}_{22})^2 + 4\mathcal{M}_{12}^2}}. \quad (2.13)$$

In the limit of small mixing, $|\alpha| \ll 1$, and assuming $\mathcal{M}_{22} > \mathcal{M}_{11}$, but not necessarily $\mathcal{M}_{22} \gg \mathcal{M}_{11}$:

$$\alpha \simeq \frac{\mathcal{M}_{12}}{\mathcal{M}_{11} - \mathcal{M}_{22}}, \quad (2.14)$$

$$V = V_1 + \alpha V_2, \quad V' = V_2 - \alpha V_1, \quad (2.15)$$

$$m_V^2 \simeq \mathcal{M}_{11} + \mathcal{M}_{12}\alpha, \quad m_{V'}^2 \simeq \mathcal{M}_{22} - \mathcal{M}_{12}\alpha. \quad (2.16)$$

2.1.1 Vector Bosons

In the charged vector boson sector, and in the (W_L, W_R) basis:

$$\mathcal{M}_\pm^2 = \frac{g^2}{4} \begin{pmatrix} v_L^2 + u^2 & -xu^2 \sin 2\beta \\ -xu^2 \sin 2\beta & x^2(v_R^2 + u^2) \end{pmatrix}. \quad (2.17)$$

In the limit of small mixing, as defined above, and in obvious notation:

$$\alpha_\pm \simeq \frac{xu^2 \sin 2\beta}{x^2(u^2 + v_R^2) - (u^2 + v_L^2)}, \quad (2.18)$$

$$m_W^2 \simeq \frac{g^2}{4} \left[(u^2 + v_L^2) - \frac{x^2 u^4 \sin^2 2\beta}{x^2(u^2 + v_R^2) - (u^2 + v_L^2)} \right], \quad (2.19)$$

$$m_{W'}^2 \simeq \frac{g^2}{4} \left[x^2(u^2 + v_R^2) + \frac{x^2 u^4 \sin^2 2\beta}{x^2(u^2 + v_R^2) - (u^2 + v_L^2)} \right]. \quad (2.20)$$

In the neutral sector, and in the $(W_L^3, W_R^3, \tilde{B})$ basis

$$\mathcal{M}_0^2 = \frac{g^2}{4} \begin{pmatrix} v_L^2 + u^2 & -xu^2 & -yv_L^2 \\ -xu^2 & x^2(v_R^2 + u^2) & -xyv_R^2 \\ -yv_L^2 & -xyv_R^2 & y^2(v_L^2 + v_R^2) \end{pmatrix}. \quad (2.21)$$

It is convenient to move to the basis defined by

$$\begin{pmatrix} A \\ Z_L \\ Z_R \end{pmatrix} = U \begin{pmatrix} W_L^3 \\ W_R^3 \\ B \end{pmatrix}, \quad (2.22)$$

where

$$U = \begin{pmatrix} \frac{xy}{\sqrt{x^2+y^2+x^2y^2}} & \frac{y}{\sqrt{x^2+y^2+x^2y^2}} & \frac{x}{\sqrt{x^2+y^2+x^2y^2}} \\ \frac{\sqrt{x^2+y^2}}{\sqrt{x^2+y^2+x^2y^2}} & -\frac{xy^2}{\sqrt{x^2+y^2}\sqrt{x^2+y^2+x^2y^2}} & -\frac{x^2y}{\sqrt{x^2+y^2}\sqrt{x^2+y^2+x^2y^2}} \\ 0 & \frac{x}{\sqrt{x^2+y^2}} & -\frac{y}{\sqrt{x^2+y^2}} \end{pmatrix}. \quad (2.23)$$

In the (A, Z_L, Z_R) basis, the mass matrix becomes block-diagonal:

$$U \mathcal{M}_0^2 U^T = \begin{pmatrix} 0 & 0 & 0 \\ 0 & \tilde{\mathcal{M}}_0^2 & \\ 0 & & \end{pmatrix}, \quad (2.24)$$

and we can identify the photon with the massless combination A . The non-vanishing block $\tilde{\mathcal{M}}_0^2$ is given by:

$$\begin{aligned} \tilde{\mathcal{M}}_0^2 &= \frac{g^2}{4(x^2 + y^2)} \\ &\times \begin{pmatrix} (u^2 + v_L^2)(x^2 + y^2 + x^2y^2) & (v_L^2y^2 - u^2x^2)\sqrt{x^2 + y^2 + x^2y^2} \\ (v_L^2y^2 - u^2x^2)\sqrt{x^2 + y^2 + x^2y^2} & x^4(u^2 + v_R^2) + 2x^2y^2v_R^2 + y^4(v_L^2 + v_R^2) \end{pmatrix}. \end{aligned} \quad (2.25)$$

Working in the limit of small mixing, as defined above:

$$\alpha_0 \simeq \frac{(v_L^2y^2 - u^2x^2)\sqrt{x^2 + y^2 + x^2y^2}}{(u^2 + v_L^2)(x^2 + y^2 + x^2y^2) - x^4(u^2 + v_R^2) - 2x^2y^2v_R^2 - y^4(v_L^2 + v_R^2)}, \quad (2.26)$$

$$\begin{aligned} m_Z^2 &\simeq \frac{g^2}{4} \frac{(x^2 + y^2 + x^2y^2)}{(x^2 + y^2)} \left[(u^2 + v_L^2) \right. \\ &\quad \left. + \frac{(v_L^2y^2 - u^2x^2)^2}{(u^2 + v_L^2)(x^2 + y^2 + x^2y^2) - x^4(u^2 + v_R^2) - 2x^2y^2v_R^2 - y^4(v_L^2 + v_R^2)} \right], \end{aligned} \quad (2.27)$$

$$\begin{aligned} m_{Z'}^2 &\simeq \frac{g^2}{4(x^2 + y^2)} \left[x^4(u^2 + v_R^2) + 2x^2y^2v_R^2 + y^4(v_L^2 + v_R^2) \right. \\ &\quad \left. - \frac{(x^2 + y^2 + x^2y^2)(v_L^2y^2 - u^2x^2)^2}{(u^2 + v_L^2)(x^2 + y^2 + x^2y^2) - x^4(u^2 + v_R^2) - 2x^2y^2v_R^2 - y^4(v_L^2 + v_R^2)} \right]. \end{aligned} \quad (2.28)$$

2.1.2 Fermions

Fermion masses arise exactly as in the SM, via the Yukawa interactions of eq. (2.6), involving fermion bilinears and the scalar doublet ϕ_L (we recall that in the FP model the scalar fields ϕ_R and ϕ_{LR} cannot have gauge-invariant couplings to fermion bilinears), thus they do not deserve any special discussion. The only point to notice is that, since fermion masses depend only on v_L , but gauge boson masses depend on all the four VEVs (v_1, v_2, v_L, v_R), the SM one-to-one correspondence between the numerical values of the fermion masses and the magnitude of the corresponding Yukawa couplings is corrected by suitable mixing parameters.

2.1.3 Scalars

A complete description of the mass spectrum and of the interactions in the scalar sector would require an explicit form of the scalar potential V_0 and its expansion around the minimum. Nevertheless, a parametrization for the mass spectrum and a discussion of some of its features can be outlined even in the absence of an explicit form for V_0 . Notice first that, out of the 16 spin-0 real degrees of freedom, 8 charged and 8 neutral, 6 (the would-be Goldstone bosons) are absorbed as longitudinal components of the massive gauge bosons: these states can be unambiguously identified in terms of the components of the multiplets ϕ_L , ϕ_R , ϕ_{LR} and of the assumed pattern of VEVs. The remaining 10 degrees of freedom, 4 charged and 6 neutral, correspond to physical spin-0 particles.

In the charged Higgs sector, the physical mass eigenstates $H_{1,2}^\pm$ can be characterized by their two masses $m_{1,2}^\pm$ and by a single mixing angle β_\pm . Calling G^\pm and G'^\pm the charged would-be Goldstone bosons associated with W and W' , respectively, we can describe the relation among $\phi^\pm \equiv (\phi_R^\pm, \phi_L^\pm, \phi_1^\pm, \phi_2^\pm)^T$ and $H^\pm \equiv (G^\pm, G'^\pm, H_1^\pm, H_2^\pm)^T$ by a matrix equation:

$$\phi^\pm = A \cdot H^\pm, \quad (2.29)$$

where the explicit form of the 4×4 orthogonal matrix A is given in appendix A.

If we assume no other sources of CP-violation besides the Kobayashi-Maskawa phase, and in particular real parameters in the scalar potential and real VEVs, the 6 physical states of the neutral Higgs sector can be divided into 2 CP-odd (H_1^0, H_2^0) and four CP-even states, and there is no mixing between the two sets. Collecting the physical CP-odd states and the neutral would-be Goldstone bosons (G^0, G'^0), associated with the neutral gauge boson mass eigenstates (Z, Z'), in a vector $H^0 \equiv (G^0, G'^0, H_1^0, H_2^0)^T$, we can relate the mass eigenstates H^0 with the interaction eigenstates $Im\phi^0 \equiv Im(\phi_R^0, \phi_L^0, \phi_1^0, \phi_2^0)^T$ in the following way:

$$\sqrt{2} \cdot Im\phi^0 = C \cdot H^0, \quad (2.30)$$

where the explicit form of the 4×4 orthogonal matrix C is given in appendix A. The neutral CP-odd sector is thus described by the two masses $m_{1,2}^0$ of $H_{1,2}^0$ and by a single mixing angle β_0 .

Finally, the neutral CP-even states $Re\phi^0 \equiv Re(\phi_R^0, \phi_L^0, \phi_1^0, \phi_2^0)^T$ can mix (6 mixing angles) to give 4 mass eigenstates with masses m_i^0 , ($i = 3, \dots, 6$). We will not give here the general parametrization for this sector. As a zeroth-order approximation, we can identify the candidate SM-like Higgs, which is bound to survive as an approximate light mass eigenstate when the scale of $SU(2)_R$ breaking and the remaining Higgs masses are pushed much above the electroweak scale. To do so, we identify three $SU(2)_L$ doublets with identical SM quantum numbers

$$\phi_L \equiv \begin{pmatrix} \phi_L^0 \\ \phi_L^- \end{pmatrix}, \quad \phi_L^1 \equiv \begin{pmatrix} \phi_1^0 \\ \phi_1^- \end{pmatrix}, \quad \phi_L^2 \equiv i\sigma^2 \begin{pmatrix} \phi_2^+ \\ \phi_2^0 \end{pmatrix} = \begin{pmatrix} \phi_2^{0*} \\ -\phi_2^- \end{pmatrix}. \quad (2.31)$$

It is easy to identify the two-dimensional subspace of linear combinations, $\chi^0 = \alpha Re \Phi_L^0 + \beta Re \Phi_1^0 + \gamma Re \Phi_2^0$, with vanishing VEVs, $\langle \chi^0 \rangle = 0$. The orthogonal linear combination, appropriately normalized, will define the SM-like Higgs h :

$$h = \frac{[v_L(\sqrt{2}Re \phi_L^0 - v_L) + v_1(\sqrt{2}Re \phi_1^0 - v_1) + v_2(\sqrt{2}Re \phi_2^0 - v_2)]}{\sqrt{v_L^2 + v_1^2 + v_2^2}}. \quad (2.32)$$

In the following sections, we shall often make the assumption that h is the only light mass eigenstate in the neutral Higgs boson sector.

2.2 Interactions

2.2.1 Gauge interactions of fermions

Charged-current gauge interactions of fermions are described by

$$\mathcal{L}_{CC} = \begin{pmatrix} J_L^{\mu+} & 0 \end{pmatrix} \begin{pmatrix} W_{\mu L}^- \\ W_{\mu R}^- \end{pmatrix} + \text{h.c.} = \begin{pmatrix} J_W^{\mu+} & J_{W'}^{\mu+} \end{pmatrix} \begin{pmatrix} W_{\mu}^- \\ W_{\mu}^{\prime-} \end{pmatrix} + \text{h.c.}, \quad (2.33)$$

where

$$J_W^{\mu+} = \cos \alpha_{\pm} J_L^{\mu+}, \quad J_{W'}^{\mu+} = -\sin \alpha_{\pm} J_L^{\mu+}, \quad (2.34)$$

and, working with quark mass eigenstates and leaving implicit the generation indices, the charged current associated with $SU(2)_L$ fermion interactions is given by:

$$J_L^{\mu+} = \frac{g}{\sqrt{2}} (\bar{e}_L \gamma^{\mu} \nu_L + \bar{d}_L \gamma^{\mu} K^{\dagger} u_L). \quad (2.35)$$

The Fermi coupling constant, as defined at the tree level from muon decay, is given by²

$$\frac{G_F}{\sqrt{2}} = \frac{g^2}{8} \left(\frac{\cos^2 \alpha_{\pm}}{m_W^2} + \frac{\sin^2 \alpha_{\pm}}{m_{W'}^2} \right). \quad (2.36)$$

²Since the couplings of the charged Higgs bosons to fermions are proportional to the relevant fermion masses, given the constraints coming from heavy-flavour decays, to be discussed in section 3, we can safely neglect the charged-Higgs contributions to muon decay.

Neutral current gauge interactions of fermions are described by

$$\mathcal{L}_{NC} = \begin{pmatrix} J_L^{\mu 3} & 0 & J_B^\mu \end{pmatrix} \begin{pmatrix} W_{\mu L}^3 \\ W_{\mu R}^3 \\ B_\mu \end{pmatrix} \quad (2.37)$$

$$= \begin{pmatrix} J_{em}^\mu & J_L^{\mu 0} & J_R^{\mu 0} \end{pmatrix} \begin{pmatrix} A_\mu \\ Z_\mu^L \\ Z_\mu^R \end{pmatrix} = \begin{pmatrix} J_{em}^\mu & J_Z^\mu & J_{Z'}^\mu \end{pmatrix} \begin{pmatrix} A_\mu \\ Z_\mu \\ Z'_\mu \end{pmatrix}, \quad (2.38)$$

where, denoting with $f_i \equiv \{e_L, e_R, \nu_L, u_L, u_R, d_L, d_R\}$ the chiral projections of the fermion fields and leaving implicit the generation indices:

$$J_L^{\mu 3} = g \sum_i T_{3L}^i \bar{f}_i \gamma^\mu f_i, \quad J_B^\mu = \tilde{g} \sum_i \tilde{Y}^i \bar{f}_i \gamma^\mu f_i, \quad (2.39)$$

$$\begin{pmatrix} J_{em}^\mu & J_L^{\mu 0} & J_R^{\mu 0} \end{pmatrix} = \begin{pmatrix} J_L^{\mu 3} & 0 & J_B^\mu \end{pmatrix} U^T, \quad (2.40)$$

and

$$J_Z = \cos \alpha_0 J_L^0 + \sin \alpha_0 J_R^0, \quad J_{Z'} = -\sin \alpha_0 J_L^0 + \cos \alpha_0 J_R^0. \quad (2.41)$$

It is convenient to write the explicit expression of the electromagnetic current:

$$J_{em}^\mu = e \sum_i Q^i \bar{f}_i \gamma^\mu f_i, \quad (2.42)$$

where

$$e = g \frac{xy}{\sqrt{x^2 + y^2 + x^2 y^2}}. \quad (2.43)$$

Notice that one recovers the SM tree-level relation $e = g \sin \theta_W$ by defining $\sin \theta_W$ as

$$\sin \theta_W \equiv \frac{xy}{\sqrt{x^2 + y^2 + x^2 y^2}}. \quad (2.44)$$

Observe also the following simple relations:

$$\frac{1}{e^2} = \frac{1}{g_R^2} + \frac{1}{g^2} + \frac{1}{\tilde{g}^2}, \quad A_\mu = \frac{e}{g} W_{L\mu}^3 + \frac{e}{g_R} W_{R\mu}^3 + \frac{e}{\tilde{g}} B_\mu. \quad (2.45)$$

The remaining two neutral currents are given by:

$$J_L^{\mu 0} = \frac{g}{\cos \theta_W} \sum_i \left(T_{3L}^i - Q^i \sin^2 \theta_W \right) \bar{f}_i \gamma^\mu f_i, \quad (2.46)$$

and

$$J_R^{\mu 0} = -\frac{gy^2}{\sqrt{x^2 + y^2}} \sum_i \tilde{Y}^i \bar{f}_i \gamma^\mu f_i. \quad (2.47)$$

Notice that, due to the fermiophobic nature of $SU(2)_R$, the two charged currents ($J_W^{\mu+}, J_{W'}^{\mu+}$) and the three neutral currents ($J_{em}^\mu, J_Z^\mu, J_{Z'}^\mu$) are not linearly independent, in contrast with the other models of table 1.

2.2.2 Other interactions

We comment now on other interaction terms that will be relevant in the discussion of the model phenomenology.

Trilinear gauge boson vertices are completely determined by gauge invariance and by the mixing angles in the gauge boson sector. Their explicit expressions in the mass eigenstate basis are collected in appendix A.

The interaction terms involving the SM-like Higgs boson h can be deduced from eqs. (2.4) and (2.6) by using eq. (2.32). In particular, the Yukawa interactions of h have exactly the same form as for the SM Higgs, and the model shares with the SM the important property that there are no tree-level FCNC induced by the scalar sector:

$$\mathcal{L}_Y^h = -\frac{1}{\sqrt{v_L^2 + v_1^2 + v_2^2}} \left(\overline{u}_L M_{diag}^U u_R + \overline{d}_R M_{diag}^D d_L + \overline{e}_R M_{diag}^E e_L \right) h + \text{h.c.} \quad (2.48)$$

It is also interesting to look at the interaction terms linear in h and bilinear in the gauge boson mass eigenstates: their explicit expressions have been collected in appendix A.

As for the Yukawa interactions of the physical charged Higgs bosons, they may play a role in some decays of heavy flavours, such as $b \rightarrow c\tau^-\overline{\nu}_\tau$ or $t \rightarrow bH_i^+$, as well as in the generation of FCNC and of non-standard contributions to $\Gamma(Z^0 \rightarrow b\overline{b})$ at the one-loop level. In view of the following discussion, it may be useful to rewrite these interactions in terms of the physical charged Higgs mass eigenstates, defined in eq. (2.29):

$$\mathcal{L}_Y^{ch} = \frac{\sqrt{2}}{v_L} \left(-\overline{d}_L K^\dagger M_{diag}^U u_R + \overline{d}_R M_{diag}^D K^\dagger u_L + \overline{e}_R M_{diag}^E \nu_L \right) \sum_{i=3,4} A_{2i} H_i^- + \text{h.c.} \quad (2.49)$$

In the following section, we shall often consider the limiting case of vanishing mixing angle in the charged gauge boson sector and of degenerate physical charged Higgs bosons:

$$\alpha_\pm = 0, \quad m_1^\pm = m_2^\pm = m_H. \quad (2.50)$$

In such a case, when dealing with processes controlled by the Yukawa interactions of the physical charged Higgs bosons, we can forget about the mixing angle β_\pm and work as if there were a single charged Higgs boson, H^\pm , with

$$\mathcal{L}_Y^{ch} = -\frac{g}{\sqrt{2}m_W} \frac{\tan\theta_W}{\sqrt{x^2 - \tan^2\theta_W}} \left(-\overline{d}_L K^\dagger M_{diag}^U u_R + \overline{d}_R M_{diag}^D K^\dagger u_L + \overline{e}_R M_{diag}^E \nu_L \right) H^- + \text{h.c.} \quad (2.51)$$

3 Phenomenology of the fermiophobic model

3.1 Approximate parametrization

Considering for the moment only gauge interactions, the model has 7 independent parameters, three gauge couplings (g, g_R, \tilde{g}) and four VEVs (v_1, v_2, v_L, v_R) . However, it is convenient to move to suitable combinations of these parameters with a more direct physical interpretation. To replace the gauge couplings, we choose the electric charge $e \equiv \sqrt{4\pi\alpha}$, the electroweak mixing angle θ_W and the ratio $x \equiv g_R/g$ between the two non-abelian couplings. The exact translation table is:

$$g = \frac{e}{s_W}, \quad g_R = \frac{ex}{s_W}, \quad \tilde{g} = \frac{ex}{\sqrt{x^2 c_W^2 - s_W^2}}, \quad (3.1)$$

where $s_W \equiv \sin \theta_W$ and $c_W \equiv \cos \theta_W$. Notice that the physical requirement $\tilde{g}^2 > 0$ corresponds to the constraint $x > \tan \theta_W \simeq 0.55$. To replace the four VEVs, we choose two gauge boson masses, for example m_Z and $m_{W'}$, and the two mixing angles, α_\pm and α_0 , assumed to be small³. We can then derive simple approximate expressions for the other relevant quantities in the gauge sector. At the lowest non-trivial order in the mixing angles, i.e. neglecting $\mathcal{O}(\alpha_{\pm,0}^2)$ terms, we find⁴:

$$m_W^2 \simeq c_W^2 m_Z^2, \quad m_{Z'}^2 \simeq \frac{x^2 c_W^2 m_{W'}^2 - s_W^4 m_Z^2}{x^2 c_W^2 - s_W^2}, \quad (3.2)$$

$$u^2 \equiv v_1^2 + v_2^2 \simeq \frac{s_W^4}{\pi \alpha x^2} m_Z^2, \quad \sin 2\beta \simeq x \frac{m_{W'}^2 - c_W^2 m_Z^2}{s_W^2 m_Z^2} \alpha_\pm, \quad (3.3)$$

$$v_L^2 \simeq \frac{s_W^2 (x^2 c_W^2 - s_W^2)}{\pi \alpha x^2} m_Z^2, \quad v_R^2 \simeq \frac{s_W^2}{\pi \alpha x^2} (m_{W'}^2 - s_W^2 m_Z^2). \quad (3.4)$$

When dealing with precision tests of the model, we must be more precise in our definitions of the input parameters. In particular, it is convenient to express the electroweak mixing angle θ_W in terms of (G_F, α, m_Z) . From eqs. (3.1) and (2.36), we get

$$m_W^2 = \frac{\mu^2}{s_W^2} \left[1 + \sin^2 \alpha_\pm \left(\frac{m_W^2 - m_{W'}^2}{m_{W'}^2} \right) \right], \quad (3.5)$$

where

$$\mu^2 \equiv \frac{\pi \alpha}{\sqrt{2} G_F}. \quad (3.6)$$

Notice that, at the lowest non-trivial order in the mixing, the relation among G_F , α , m_W and s_W remains the same as in the SM. To eliminate m_W in favour of m_Z in eq. (3.5), we proceed as in the SM, defining

$$\rho \equiv \frac{m_W^2}{m_Z^2 c_W^2}. \quad (3.7)$$

³The allowed range for the mixing angles α_\pm and α_0 is not completely arbitrary: once $(x, m_{W'})$ are given, and $(\alpha, m_Z, \sin \theta_W)$ extracted from experiment, $|\alpha_\pm|$ and $|\alpha_0|$ are bounded from above, as can be seen by inspecting the vector boson mass matrices.

⁴We should warn the reader that, for very large values of x or $m_{W'}$, subleading terms in the (α_0, α_\pm) expansion may become non-negligible. For our numerical results we will always use the complete formulae.

In the limit of small mixing, we find:

$$\rho \equiv 1 + \Delta\rho = 1 + \Delta\rho_W + \Delta\rho_Z, \quad (3.8)$$

where

$$\Delta\rho_W \simeq -\alpha_\pm^2 \frac{m_{W'}^2 - m_W^2}{m_W^2}, \quad \Delta\rho_Z \simeq \alpha_0^2 \frac{m_{Z'}^2 - m_Z^2}{m_Z^2}. \quad (3.9)$$

By combining eqs. (3.5) and (3.7), we obtain:

$$s_W^2 \simeq \bar{s}^2 - \frac{\bar{c}^2 \bar{s}^2}{(\bar{c}^2 - \bar{s}^2)} \Delta\rho_{eff}, \quad (3.10)$$

where

$$\bar{s}^2 = \frac{1}{2} - \sqrt{\frac{1}{4} - \frac{\mu^2}{m_Z^2}} \quad (3.11)$$

corresponds to the well-known tree-level SM relation, and

$$\Delta\rho_{eff} \simeq \Delta\rho - \alpha_\pm^2 \left(\frac{m_W^2 - m_{W'}^2}{m_{W'}^2} \right) \simeq \alpha_0^2 \frac{m_{Z'}^2 - m_Z^2}{m_Z^2} - \alpha_\pm^2 \frac{(m_{W'}^2 - m_W^2)^2}{m_W^2 m_{W'}^2} \quad (3.12)$$

parametrizes the deviation from it, still at the classical level. Eq. (3.10) allows to express θ_W in terms of the input parameters (G_F, α, m_Z) , plus corrections vanishing in the limit of zero mixing angles. In summary, we can use as independent parameters (G_F, α, m_Z) , the same input quantities of the SM precision tests, plus α_\pm , α_0 , $m_{W'}$ and x .

There are two combinations of these parameters which are particularly relevant to our analysis. The first one is the ratio g/c_W appearing in the expression of the neutral current J_L^0 , eq. (2.46). In the limit of small mixing angle:

$$\frac{g^2}{c_W^2} = 4\sqrt{2}G_F m_Z^2 (1 + \Delta\rho_{eff}). \quad (3.13)$$

This relation shows that the strength of the neutral current gets corrected by the same parameter, $\Delta\rho_{eff}$, that modifies the weak mixing angle θ_W . Of course, quantum corrections also modify the classical SM relations and, in particular, may contribute to the parameter $\Delta\rho_{eff}$ of eq. (3.12): we will discuss this issue later on. The second quantity of interest is the ratio m_W/m_Z , which satisfies the relation:

$$\frac{m_W^2}{m_Z^2} \left(1 - \frac{m_W^2}{m_Z^2} \right) = \frac{\mu^2}{m_Z^2 (1 - \Delta r)}, \quad (3.14)$$

with

$$\Delta r \simeq -\frac{\bar{c}^2}{\bar{s}^2} \Delta\rho + \alpha_\pm^2 \left(\frac{m_W^2 - m_{W'}^2}{m_{W'}^2} \right). \quad (3.15)$$

In the remaining sections we will allow the parameter x to vary in a wide range, starting from its lower bound, $\tan \theta_W$, up to values as large as 20. We may wonder about the properties of the theory in the large x regime (similar considerations have been recently

made, in a similar context, in ref. [6]). In particular, we would like to maintain control over the predictions that are relevant to our analysis, even in the presence of the strong interactions associated with g_R . It turns out that, when x is large, the states of the model split into two sectors. The first sector includes the new vector bosons W' and Z' and the scalar mass eigenstates having projections along the multiplets ϕ_R and ϕ_{LR} . This sector experiences the strong interaction related to the large g_R coupling. The second sector comprises the ordinary vector bosons, the fermions and the rest of the scalar sector. The interactions among these states do not grow with x , at least in the case of vanishing mixing angles α_0 and α_{\pm} , which represents, as we shall see, a good approximation to the realistic case. Finally, when considering processes involving only ordinary particles, which belong to the second sector, the corrections induced by the states of the first sector are bounded in the large x limit, for vanishing α_0 and α_{\pm} . This structure guarantees that, as long as we work at energies below the threshold of particle production in the first sector, the strong interaction cannot propagate to the states of the second sector. We will sometimes consider the possibility of producing real W' and Z' . In this case a very large value of x might lead to violation of perturbative unitarity. We restrict our numerical analysis to $x \lesssim 20$, corresponding to $g_R \lesssim 13$.

3.2 Tree-level fit to electroweak data

A first important constraint on the parameter space of the model comes from the comparison with the electroweak data collected at the Z peak, the ratio m_W/m_Z and the low-energy data from neutrino-hadron scattering and atomic parity violation experiments. A recent compilation of these data [7] is shown in table 3. In general, the deviation from the SM prediction of the generic observable of table 3 depends on the parameters α_0 , α_{\pm} , x and $m_{W'}$. The main dependence comes through the combination $\Delta\rho_{eff}$, which modifies both the electroweak mixing angle θ_W and the strength of the neutral current, and through the combination $\alpha_0 y^2 / \sqrt{x^2 + y^2}$, which controls the amount of contamination of the ordinary neutral current J_L^0 by the new current J_R^0 . Exceptions to this rule are the low-energy observables $g_{L,R}^2$, associated with neutrino-hadron scattering (and not to be confused with the $SU(2)$ coupling constants) and Q_W , associated with atomic parity violation, which are also affected by direct Z' exchange, and the ratio m_W/m_Z , which is corrected by Δr . The explicit form of these corrections can be easily obtained, following for instance the procedure outlined in refs. [8], and will not be reported here. To test the model against the electroweak data, we have performed a fit to the 14 observables of table 3. The theoretical predictions of the model have been obtained by adding to the SM predictions, radiative corrections included, the appropriate deviations, as computed at the classical level in the FP model. A χ^2 minimization procedure determines the best values and the errors for the parameters of the fit, to be chosen among α_0 , α_{\pm} , x and $m_{W'}$. Besides the input values for (G_F, α, m_Z) , the SM one-loop predictions also depend on the top mass m_t , the Higgs mass m_h and the strong coupling constant α_s , which will be kept fixed. The Higgs

Quantity	Exp. values
$\Gamma_Z(\text{MeV})$	2494.7 ± 2.6
$R_l = \Gamma_h/\Gamma_l$	20.783 ± 0.029
$\sigma_h(nb)$	41.489 ± 0.055
$R_b = \Gamma_b/\Gamma_h$	0.2177 ± 0.0011
$R_c = \Gamma_c/\Gamma_h$	0.1722 ± 0.0053
m_W/m_Z	0.8814 ± 0.0008
\mathcal{A}_l	-0.1512 ± 0.0023
\mathcal{A}_b	-0.897 ± 0.047
\mathcal{A}_c	-0.623 ± 0.085
A_{FB}^b	0.0985 ± 0.0022
A_{FB}^c	0.0735 ± 0.0048
$Q_W(Cs)$	-72.08 ± 0.93
g^2	0.3017 ± 0.0033
g_R^2	0.0326 ± 0.0033

Table 3: *Experimental values for the electroweak observables used in our fit.*

boson h is identified here with what we defined as SM-like Higgs in eq. (2.32). Additional dependences of the radiative corrections upon the other scalar particles and the additional gauge bosons will be addressed separately in the following section.

To keep the number of fit parameters reasonably small, we fix the x parameter by choosing the following set of representative values: 0.6, 1, 2.5, 5, 15. Then we observe that the fit is quite insensitive to the W' mass: $m_{W'}$ is determined with a huge error. In view of this, we prefer to keep also $m_{W'}$ fixed in the minimization procedure, and we assign to it some representative values in the range 100–1000 GeV. The final results are displayed in tables 4 and 5, where we report the best values and the 1σ errors for α_0 (α_{\pm}) in units of 10^{-3} . From table 4 we see that α_0 scales approximately as x , which confirms the fact that the deviations for the LEP observables, beyond $\Delta\rho_{eff}$, depend only on the combination $\alpha_0 y^2/\sqrt{x^2 + y^2}$. We also notice that, most of the times, the value of α_{\pm} , although affected by a large error, is very close to zero. This can be understood in terms of the contribution to $\Delta\rho_{eff}$ proportional to α_{\pm}^2 . This contribution, detailed in eq. (3.12), is always negative. On the other hand, for the chosen values of m_t and m_h , the data require a positive $\Delta\rho_{eff}$ and force the α_{\pm}^2 contribution to vanish.

For small values of x , ($x < 5$), α_0 is also small, $\mathcal{O}(10^{-3})$, and its contribution to $\Delta\rho_{eff}$

$m_{W'}$ (GeV)	$x = 0.6$	$x = 1$	$x = 2.5$	$x = 5$	$x = 15$
100	- -	- -	- -	-11.3 ± 5.2 (0 ± 29)	-34.7 ± 13.0 (0 ± 37)
200	- -	- -	-5.9 ± 2.4 (0 ± 8)	-10.6 ± 3.3 (0 ± 14)	-23.7 ± 15.7 (-18.0 ± 18.9)
500	-0.6 ± 0.2 (0 ± 3)	-2.0 ± 0.8 (0 ± 3)	-4.4 ± 1.2 (0 ± 10)	-8.2 ± 5.8 (-5.9 ± 6.9)	-23.6 ± 15.1 (-20.5 ± 13.8)
1000	-0.6 ± 0.2 (0 ± 2)	-1.7 ± 0.5 (0 ± 3)	-4.0 ± 2.9 (-3.0 ± 3.4)	-8.2 ± 5.7 (-6.9 ± 5.4)	-23.6 ± 13.9 (-20.7 ± 12.3)

Table 4: *Best values and 1σ errors for α_0 (α_{\pm}) in units of 10^{-3} , for the indicated values of x and $m_{W'}$, and: $m_t = 175$ GeV, $m_h = 300$ GeV, $\alpha_s(m_Z) = 0.118$. Here 0 stands for a value smaller than 10^{-6} . Where no value is indicated, the minimum χ^2 is larger than 25.*

remains within the allowed experimental range even for very large $m_{Z'}$ values. On the contrary, for large values of x , ($x > 5$), the best value of α_0 is close to 10^{-2} . In this case, when large $m_{W'}$ or $m_{Z'}$ are considered, the positive α_0^2 contribution to $\Delta\rho_{eff}$ is too large and a compensating negative term is required. This explains why, for large x and $m_{W'}$, the preferred values for α_{\pm} are non-vanishing and approximately equal in size to α_0 .

$m_{W'}$ (GeV)	$x = 0.6$	$x = 1$	$x = 2.5$	$x = 5$	$x = 15$
100	- -	- -	- -	-0.5 ± 5.7 (-47.2 ± 21.3)	-1.2 ± 17.0 (-47.0 ± 21.4)
200	- -	- -	-1.0 ± 2.9 (-12.3 ± 4.9)	-1.9 ± 5.9 (-12.3 ± 5.2)	-5.6 ± 17.8 (-13.2 ± 9.3)
500	-0.2 ± 0.3 (-4.4 ± 1.6)	-0.4 ± 1.0 (-4.3 ± 1.7)	-1.0 ± 2.9 (-4.4 ± 1.9)	-2.0 ± 5.9 (-4.6 ± 3.0)	-6.4 ± 17.4 (-7.1 ± 12.7)
1000	-0.1 ± 0.3 (-2.1 ± 0.8)	-0.4 ± 1.0 (-2.1 ± 0.9)	-1.0 ± 2.9 (-2.3 ± 1.5)	-2.0 ± 5.8 (-2.8 ± 3.7)	-6.5 ± 15.7 (-6.1 ± 13.1)

Table 5: *Best values and 1σ errors for α_0 (α_{\pm}) in units of 10^{-3} , for the indicated values of x and $m_{W'}$, and: $m_t = 175$ GeV, $m_h = 100$ GeV, $\alpha_s(m_Z) = 0.118$. The χ^2 minimum is between 17 and 25. Where no value is indicated, the minimum χ^2 is larger than 25.*

In table 5 we present the results for $m_t = 175$ GeV, $m_h = 100$ GeV and $\alpha_s(m_Z) = 0.118$. Notice that, for W' masses in the chosen range, the fit is insensitive to $m_{W'}$. Only when x is small, the χ^2 minimum indicates that large values of $m_{W'}$ are preferred due to the

potentially large contributions to the low-energy observables via direct Z' exchange (this also happens in the case discussed before). Moreover, α_0 is, to a large extent, independent of $m_{W'}$, and scales approximately with x . Finally, for $x < 5$ the best value of α_{\pm} is insensitive to x and is smaller for larger $m_{W'}$ values. Indeed, for the chosen values of m_t and m_h , the SM contribution to $\Delta\rho$ tends to exceed the experimentally allowed one. This excess is in turn compensated by the negative contribution coming from $\Delta\rho_W$ of eq. (3.9), with a suitable combination of α_{\pm} and $m_{W'}$. This also explains why the central value of α_{\pm} is non vanishing, contrary to the case of table 4. When x gets large ($x > 5$), the situation is similar to that discussed for $m_h = 300$ GeV and analogous considerations apply.

As explained above, in performing the fit we have only considered the SM one-loop corrections, neglecting the radiative corrections which may be originated by the additional sectors of the FP model coupled to the SM. The validity of such an approximation will be discussed in the next subsection. For the moment we can observe that, in the absence of new one-loop corrections quadratically dependent on combinations of particle masses, the numerical difference between the results of tables 4 and 5 may be regarded as indicative of the theoretical uncertainty underlying the present discussion.

In summary, comparison with electroweak precision data allows for mixing angles (α_0, α_{\pm}) in the range $10^{-3} - 10^{-2}$, depending on the value of x : larger mixing for larger x . The allowed mass range for W' and Z' is broad, and even relatively light new vector bosons can be acceptable, except for small values of x .

3.3 One-loop corrections from the scalar sector

In performing the fit described in the previous section, we have tacitly assumed that the most important quantum corrections to the electroweak observables in the FP model are the SM ones. In other words, we have neglected all the loop corrections due to the additional particles of the FP model. In view of the precision reached by the present electroweak data, we would like to comment here about the possible validity of such an approximation, considering the one-loop contributions to $\Delta\rho$ and to $R_b \equiv \Gamma_b/\Gamma_h$ due to the scalar sector of the FP model.

3.3.1 $\Delta\rho$

In general, we expect that the most dangerous non-SM radiative correction may be the one-loop contribution to $\Delta\rho$ due to the scalar sector of the FP model. Indeed, on dimensional grounds this contribution can depend quadratically upon the masses of the scalar particles, and even for masses within few hundred GeV, it can easily reach the by now intolerable percent level. Therefore, it is important to look for those configurations of the scalar sector that could appropriately deplete such correction. It is not difficult to figure out that such configurations indeed exist, in some particular limit of the model (for a generalization to larger groups, see [9]).

Consider for instance the large v_R limit, at fixed values of the remaining parameters. In this limit, the $SU(2)_R$ symmetry is broken at a scale much higher than the $SU(2)_L \otimes U(1)_Y$ breaking scale, $G_F^{-1/2}$, and it makes sense to consider an effective theory valid at energies close to $G_F^{-1/2}$. The effective theory possesses an $SU(2)_L \otimes U(1)_Y$ gauge invariance and, if the physical scalar contained in the ϕ_R multiplet is an approximate mass eigenstate, with a mass of order v_R , the surviving light scalar sector includes only the multiplets ϕ_L and ϕ_{LR} . From the point of view of the low-energy gauge symmetry, these are just three $SU(2)_L$ doublets, with the same hypercharge, which we have already denoted by $(\phi_L, \phi_L^1, \phi_L^2)$ in eq. (2.31). Their linear combination with non-vanishing VEV, eq. (2.32), corresponds to the SM-like Higgs h , whilst the two orthogonal combinations are just additional matter multiplets with no rôle in the symmetry breaking mechanism. In particular, if the physical components of these multiplets are approximate mass eigenstates, then it is very simple to compute the corresponding one-loop contribution to the $\Delta\rho$ parameter. We obtain the usual SM Higgs contribution, which is at most logarithmic in the Higgs mass, plus the contribution of two extra scalar doublets, which reads:

$$\begin{aligned} \Delta\rho = & \frac{g^2}{64\pi^2 m_W^2} \left\{ m_1^{\pm 2} - g(m_5, m_1^0) + [g(m_1^\pm, m_5) + g(m_1^\pm, m_1^0)] \right. \\ & \left. + m_2^{\pm 2} - g(m_6, m_2^0) + [g(m_2^\pm, m_6) + g(m_2^\pm, m_2^0)] \right\}, \end{aligned} \quad (3.16)$$

where

$$g(m_i, m_j) = \frac{m_i^2 m_j^2}{m_j^2 - m_i^2} \log \frac{m_i^2}{m_j^2}, \quad (3.17)$$

and we have denoted by m_5 and m_6 the masses of the two neutral CP-even bosons that sit in the same doublets with (H_1^\pm, H_1^0) and (H_2^\pm, H_2^0) , respectively. From the previous expression one recovers immediately the well-known result that, if there are no mass splittings ($m_1^\pm = m_1^0 = m_5$ and $m_2^\pm = m_2^0 = m_6$) between the scalars inside each doublet, the quadratic contribution to $\Delta\rho$ vanishes for arbitrary values of the common scalar masses. We also notice that, in the large v_R limit, the masses of the observed gauge bosons are given by:

$$m_W^2 = \frac{g^2}{4}(v_L^2 + u^2), \quad m_Z^2 = \frac{g^2}{4}(v_L^2 + u^2) \frac{x^2 + y^2 + x^2 y^2}{x^2 + y^2}, \quad (3.18)$$

and the tree level ρ parameter is exactly equal to one.

Indeed, the above cancellation of $\Delta\rho$, both at tree-level and in the one-loop approximation, may be related to the same custodial symmetry [10] that protects the ρ parameter in the SM. In the considered limit, the multiplet ϕ_R , containing the would-be Goldstone bosons absorbed by W' , Z' and a neutral physical scalar, is a singlet of the custodial $SU(2)$ and does not affect the ρ parameter. Of the remaining doublets, those with non vanishing VEVs are doublets of the custodial $SU(2)$ and should be degenerate to preserve $\rho = 1$; the one acquiring a VEV splits in a triplet plus a singlet, as in the SM.

There are other configurations of the scalar sector that are reminiscent of a custodial symmetry. We observe that, when $y = 0$ and $v_1 = v_2 = v$, the mass matrices in the neutral

and in the charged sectors coincide. In particular, in this simplified situation, the photon corresponds to the B gauge boson and the massive gauge bosons are admixtures of the W_L^i, W_R^i states. Moreover, the mixing angles α_0 and α_{\pm} are the same, which allows to discuss in simple terms the interactions of the physical W and Z with the scalar particles. To this purpose, it is instructive to express the covariant derivatives acting on the scalar fields as functions of the mass eigenstates W and Z :

$$\begin{aligned} D_{\mu}\phi_L &= (\partial_{\mu} - ig \cos \alpha W_{\mu}^a \frac{\tau^a}{2})\phi_L + \dots, \\ D_{\mu}\phi_R &= (\partial_{\mu} - igx \sin \alpha W_{\mu}^a \frac{\tau^a}{2})\phi_R + \dots, \\ D_{\mu}\phi_{LR} &= \partial_{\mu}\phi_{LR} - ig \cos \alpha W_{\mu}^a \frac{\tau^a}{2}\phi_{LR} + igx \sin \alpha W_{\mu}^a \phi_{LR} \frac{\tau^a}{2} + \dots \end{aligned} \quad (3.19)$$

where we have denoted with α the common value $\alpha_0 = \alpha_{\pm}$, with W_{μ}^a the mass eigenstates (W_{μ}^{\pm}, Z_{μ}), and the dots stand for terms containing the W' and Z' fields. Notice that, if $\cos \alpha = x \sin \alpha$, then, as far as the scalar sector is concerned, it is possible to define an $SU(2)_W$ transformation under which ϕ_L and ϕ_R transform as complex doublets, whereas ϕ_{LR} decomposes in a complex triplet ϕ_3 plus a complex singlet ϕ_1 .

It is also useful to think of ϕ_L and ϕ_R as doublets of an additional global $SU(2)_X$, acting on the right of the multiplets, when written as 2×2 matrices:

$$\phi_{L,R} \leftrightarrow \begin{pmatrix} \phi_{L,R}^0 & -\phi_{L,R}^+ \\ \phi_{L,R}^- & (\phi_{L,R}^0)^* \end{pmatrix} \quad (3.20)$$

The multiplets ϕ_3 and ϕ_1 are singlets under $SU(2)_X$. The assumed pattern of VEV's breaks $SU(2)_W \otimes SU(2)_X$ down to the diagonal subgroup $SU(2)_C$, which defines a custodial symmetry.

The multiplets with a non-vanishing VEV are now ϕ_L, ϕ_R and, due to the $v_1 = v_2 = v$ condition, ϕ_1 . The would-be Goldstone bosons eaten up by the massive W and Z are contained in the ϕ_L, ϕ_R doublets, whereas those absorbed by the W' and Z' particles are generically shared by all the multiplets. If we further require $v \gg v_L, v_R$, then the Goldstone modes related to W' and Z' are only contained in $\phi_3 \oplus \phi_1$. The physical scalars in the spectrum, classified according to $SU(2)_C$, are now: a complex doublet, linear combination of ϕ_L and ϕ_R with vanishing VEV, a neutral scalar belonging to the combination of ϕ_L and ϕ_R with non-vanishing VEV and singlet under $SU(2)_C$, a real triplet coming from ϕ_3 after subtracting the Goldstones and, finally, a complex singlet ϕ_1 . This physical spectrum corresponds, in our conventions of appendix A, to $\beta_{\pm} = \beta_0 = 0$. The overall one-loop contribution to $\Delta\rho$ coming from the scalar sector will now be that of a complex doublet plus a real triplet of matter particles. An explicit computation gives:

$$\begin{aligned} \Delta\rho &= \frac{x^2}{16\pi^2 v_L^2 (1+x^2)} \left[m_1^{\pm 2} - g(m_5, m_1^0) + g(m_1^{\pm}, m_5) \right. \\ &\quad \left. + g(m_1^{\pm}, m_1^0) + 2(m_2^{\pm 2} + m_6^2) + 4g(m_2^{\pm}, m_6) \right], \end{aligned} \quad (3.21)$$

where m_5 and m_6 are the masses of the neutral CP-even states in the linear combination of ϕ_L and ϕ_R with vanishing VEV and in ϕ_3 , respectively. This contribution vanishes for degenerate multiplets, that is for $m_1^\pm = m_1^0 = m_5$ and $m_2^\pm = m_6$. Moreover, we have explicitly verified that, when $y \neq 0$, the previous result may receive only logarithmic corrections, as is the case for the SM. In this case the mixing angles in the charged and neutral sector are no longer the same and the condition $\cos \alpha = x \sin \alpha$ should be replaced by $v_R = v_L/x$. To summarize, when $v_1 = v_2 = v \gg v_R = v_L/x$, one-loop corrections to the ρ parameter quadratic in the scalar masses can be avoided, if the physical scalars fit in appropriate degenerate multiplets of a custodial $SU(2)_C$. In this configuration (before taking the large v limit), the exact tree-level masses for the gauge bosons become particularly simple

$$\begin{aligned} m_W^2 &= \frac{g^2 v_L^2}{4}, & m_Z^2 &= \frac{g^2 v_L^2}{4} \frac{(x^2 + y^2 + x^2 y^2)}{x^2}, \\ m_{W'}^2 &= m_{Z'}^2 = \frac{g^2}{4} (v_L^2 + 2v^2(1 + x^2)), \end{aligned} \quad (3.22)$$

and the mixing angles in the gauge boson sector are simply given by:

$$\tan \alpha_\pm = \frac{1}{x}, \quad \tan \alpha_0 = \frac{1}{\sqrt{x^2 c_W^2 - s_W^2}}. \quad (3.23)$$

From the vector boson masses we find a tree-level ρ parameter equal to:

$$\rho = \frac{x^2}{x^2 + y^2} = 1 - \frac{s_W^2}{x^2 c_W^2} \quad (3.24)$$

To suppress the unacceptable contribution to $\Delta\rho$, one should consider large values of the x parameter. In turn, a large g_R coupling constant does not necessarily imply large observable effects on the ordinary particles, since the mixing angles scale as $1/x$.

By analysing the explicit expression of the one-loop contribution to $\Delta\rho$ from the scalar sector, we have also found other solutions giving a one-loop vanishing result. In particular, we would like to mention a variant of the solution discussed above, corresponding to the choices: $v_1 = v_2 = v$, $v_R = v_L/x$ and $\tan \beta_\pm = \tan \beta_0 = -m_{W'}/m_W$. In this case, we no longer require $v \gg v_R$, but we fix the mixing angles in the scalar sector to a particular non-vanishing value. We obtain:

$$\begin{aligned} \Delta\rho &= \frac{x^2}{16\pi^2 v_L^2 (1 + x^2)} \left\{ 2(m_1^{\pm 2} + m_5^2) + 4g(m_5, m_1^\pm) \right. \\ &\quad + (1 - \frac{1}{\tan \beta^2})^2 [m_2^{\pm 2} - g(m_2^0, m_6) + g(m_2^\pm, m_6) + g(m_2^\pm, m_2^0)] \\ &\quad + \frac{1}{\tan \beta^2} [2(m_2^{\pm 2} + m_2^{0 2}) + 4g(m_2^0, m_2^\pm)] \\ &\quad \left. + (\frac{1}{\tan \beta^2} - \frac{1}{\tan \beta^4}) (g(m_2^\pm, m_4) - g(m_2^0, m_4)) \right\} \end{aligned} \quad (3.25)$$

This contribution vanishes when $m_1^\pm = m_5$ and $m_2^0 = m_2^\pm$. The tree-level ρ parameter is still given by eq. (3.24) and agreement with data requires large x values. To establish an allowed range for x we have fitted again the electroweak data of table 3 in this special case. The two defining conditions reduce to two the number of independent parameters, that we have chosen to be x and $m_{W'}$. As before we have fixed $m_t = 175$ GeV, $\alpha_s(m_Z) = 0.118$ and we have considered the two cases $m_h = 100$ GeV and $m_h = 300$ GeV. We have found no sensitivity of the fit to the $m_{W'}$ parameter, which has been kept fixed to several values in the range (100, 1000) GeV. We found no significant improvement with respect to the SM case, recovered in the large x limit, and $x > 16$ at the 2σ level.

Notice that in the present case a large x does not necessarily mean large W' and Z' masses. From eq. (3.22) we see that a large x can be compensated by a small v . Indeed, this is the only case we found where a one-loop vanishing contribution to $\Delta\rho$ from the scalar sector can be compatible with relatively light new vector bosons.

We have checked that, in all configurations of VEVs described above where the quadratic scalar contribution vanishes, also the contribution quadratic in the mass of the new gauge bosons W' , Z' cancels. The cancellation always occurs inside each individual self-energy ($\Sigma_{WW}, \Sigma_{ZZ}, \Sigma_{\gamma Z}$), and involves not only diagrams with gauge particles running in the loop, but also those with gauge and scalar internal lines (only G'). The remaining contribution is at most logarithmic in the W', Z' masses.

It is interesting to note that, when $v_1 = v_2 = v$, $v_R = v_L/x$, it is possible to find contact with the so-called BESS model [11], which couples a triplet of new vector bosons to the SM particles by means of a non-renormalizable, effective lagrangian. The model, designed to describe general features of schemes of dynamical breaking of the electroweak symmetry, possesses no physical scalar particle. The relation of BESS to the FP model should then be looked for in the gauge boson and fermion sectors. BESS is described, in its minimal form, by 5 parameters (see ref. [11]): a VEV f , three gauge coupling constants g , g' and g'' and a dimensionless coupling α . The particular case we are dealing with is also characterized by 5 parameters, due to the 2 conditions among the VEVs imposed to screen $\Delta\rho$ from large one-loop corrections. We can take g , x , y , v and v_R as free parameters. It turns out that generic values of these parameters do not reproduce the relations of the BESS model. It is however sufficient to require the additional condition $v_R = \sqrt{2}v$ in order to recover the same results of BESS for the vector boson masses, the mixing angles and the fermionic interaction terms. On its side, the BESS model is constrained by the additional relation $\alpha = 2g^2/(2g^2 + g''^2)$, which restricts to 4 the number of independent parameters. For the interested reader, we collect in table 3.3.1 the dictionary from the BESS model to the present one, both subject to the supplementary conditions needed to relate the models. By relaxing the condition $v_R = v_L/x$, it is possible to find a one-to-one correspondence between the two models in the full 5-fold parameter space, as already noticed in the last of refs. [3]. In this case, however, the one-loop contributions to $\Delta\rho$ from the scalar sector are quadratic in the scalar masses and hardly reconcilable with the data.

BESS model	Present model
α	$\frac{1}{(1+2x^2)}$
f	$v\sqrt{1+2x^2}$
g''	$2gx$
g	g
g'	\tilde{g}

Table 6: *Translation table between the BESS model, subject to the condition $\alpha = 2g^2/(2g^2 + g''^2)$ and the present model, subject to the conditions $v_1 = v_2 = v$, $v_R = v_L/x = \sqrt{2}v$.*

3.3.2 R_b

At the classical level, the SM prediction for R_b can be modified by mixing effects in the gauge boson sector, as accounted for in our tree-level fit to electroweak precision data. We have explicitly verified that, in the region of parameter space allowed by our fit, the shift in the predicted value of R_b with respect to its SM value is always negligible, i.e. smaller in absolute value than 10^{-4} . This suggests that non-negligible (and non-SM) loop corrections to R_b may possibly come only from loops involving the extra scalar particles of the FP model. Loops involving the exchange of neutral Higgs bosons are controlled by couplings proportional to the b -quark mass, and cannot give large effects. Similarly, the one-loop W' contribution is suppressed by $(\alpha_{\pm})^2$. The only contributions that deserve a more accurate study are those associated with the exchange of virtual charged Higgs bosons. For simplicity, we work in the limiting case of eqs. (2.50) and (2.51). We can then express the additional contribution to R_b due to charged Higgs exchange as [12]

$$\Delta R_b \simeq (R_b)_{SM} \times 0.78 \times \frac{\alpha_W}{2\pi} \frac{v_L}{v_L^2 + v_R^2} \times F_H, \quad (3.26)$$

where $(R_b)_{SM} \simeq 0.2158$ is the SM prediction, $\alpha_W \equiv 4\pi g^2$ and

$$v_L = -\frac{1}{2} + \frac{1}{3} \sin^2 \theta_W, \quad v_R = \frac{1}{3} \sin^2 \theta_W. \quad (3.27)$$

The function F_H , associated with the top-Higgs loops, depends on the common mass m_H of the charged Higgs bosons and on their dominant coupling to top and bottom quarks, eq. (2.51):

$$\lambda_H = \frac{m_t}{\sqrt{2}m_W} \frac{\tan \theta_W}{\sqrt{x^2 - \tan^2 \theta_W}}, \quad (3.28)$$

and reads

$$\begin{aligned} F_H = & \left\{ b_1(m_H, m_t) v_L - c_0(m_t, m_H) v_L^{(H)} + m_t^2 c_2(m_H, m_t) v_L^{(t)} \right. \\ & \left. + \left[m_Z^2 c_6(m_H, m_t) - \frac{1}{2} - c_0(m_H, m_t) \right] v_R^{(t)} \right\} \lambda_H^2. \end{aligned} \quad (3.29)$$

The functions b_1 , c_0 , c_2 and c_6 can be found, for example, in the appendix of ref. [13], and

$$v_L^{(t)} = \frac{1}{2} - \frac{2}{3} \sin^2 \theta_W, \quad v_R^{(t)} = -\frac{2}{3} \sin^2 \theta_W, \quad v_L^{(H)} = -\frac{1}{2} + \sin^2 \theta_W. \quad (3.30)$$

Fixing $m_t = 175$ GeV, we have explored the possible values of ΔR_b as functions of m_H

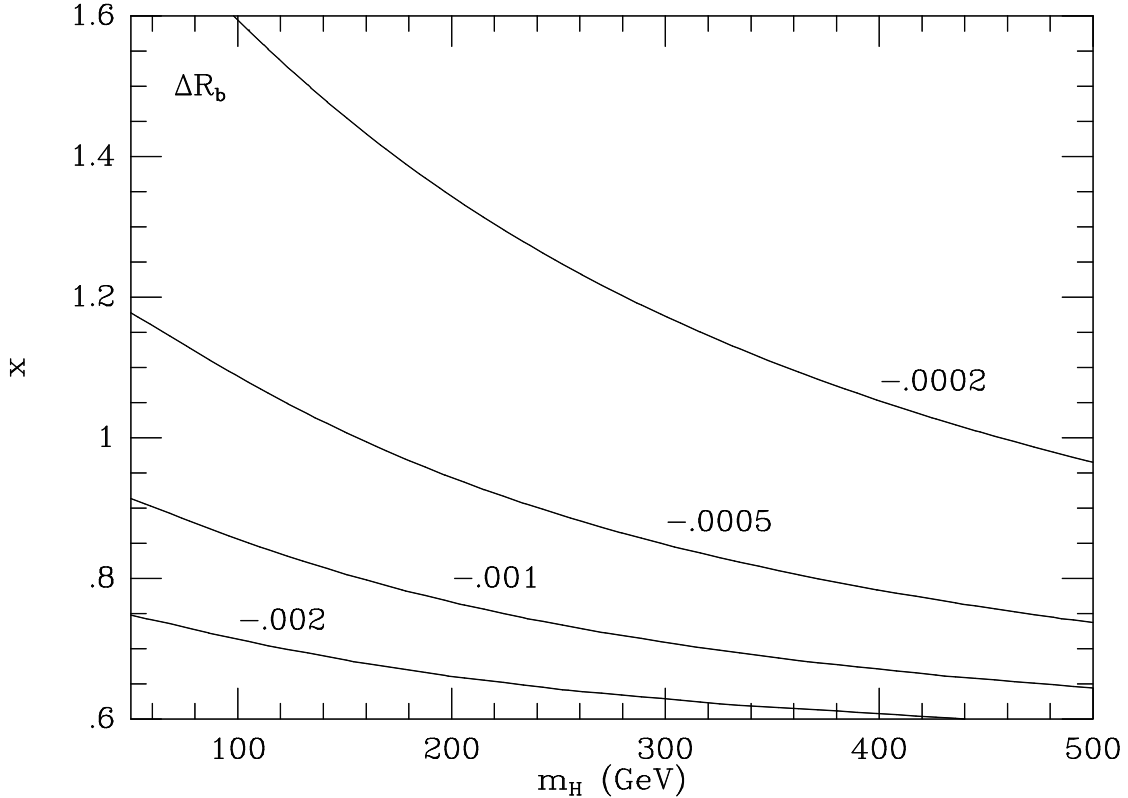


Figure 1: *Contours of ΔR_b in the (m_H, x) plane.*

and x , as shown by the contours in fig. 1. It is important to notice that in the case under consideration ΔR_b is always negative, and sizeable effects can be obtained for small m_H and x close to $\tan \theta_W$, corresponding to a strong λ_H coupling. Since the world average for R_b , given in table 3, is 1.75σ in excess with respect to the SM prediction, with an experimental situation still in rapid evolution, we choose $\Delta R_b > -0.001$ as a tentative bound. We can then see that a significant region of the (m_H, x) plane can already be excluded.

3.4 Contributions to flavour-changing processes

In general, models based on the gauge group $SU(2)_L \times SU(2)_R \times U(1)_{\tilde{Y}}$ are very strongly constrained by experimental data from flavour physics, in particular by FCNC processes [14]. In this respect, the FP model has a privileged status, since it automatically guarantees

the absence of FCNC at tree-level and the suppression of loop-induced effects, thanks to the fact that the unmixed $SU(2)_R$ gauge bosons and the (ϕ_{LR}, ϕ_R) Higgs bosons do not have direct couplings to the matter fermions.

Choosing $|\alpha_{\pm}| < 0.01$, as suggested by our fit to electroweak observables, and $m_{W'} \gtrsim m_W$, we can estimate a negligible one-loop contribution to the relevant observables from W' exchange. In the present discussion such contribution can be safely omitted, and our focus will be on the charged Higgs boson exchanges that, for flavour-changing phenomena, dominate the one-loop corrections of non-standard origin whenever they are non-negligible. To gauge the typical effects from the charged scalar sector we will work in the limit of eqs. (2.50–2.51).

Before moving to loop-induced FCNC processes, it is useful to review the limits on the charged Higgs sector that come from tree-level charged-current processes, such as heavy flavour decays. The process $b \rightarrow c \tau \nu_\tau$, that originates non-trivial constraints in other multi-Higgs models [15], is of no use in the FP model, since the Yukawa couplings proportional to the b and τ masses are always much smaller than those proportional to the t mass. This is an obvious consequence of the fact that in the FP model only ϕ_L is coupled to fermions.

Interesting limits can instead be obtained by considering the decay $t \rightarrow bH^+$, which competes with the SM channel $t \rightarrow bW^+$. In the limiting case of eqs. (2.50) and (2.51), the partial widths for $t \rightarrow bH^+$ and $t \rightarrow bW^+$ read:

$$\Gamma(t \rightarrow bH^+) = \frac{\sqrt{[m_t^2 - (m_H + m_b)^2][m_t^2 - (m_H - m_b)^2]}}{16\pi m_t^3} \cdot \mathcal{A}_H, \quad (3.31)$$

$$\mathcal{A}_H = \frac{g^2}{4m_W^2} \frac{\tan^2 \theta_W}{x^2 - \tan^2 \theta_W} \left[(m_t^2 + m_b^2 - m_H^2)(m_b^2 + m_t^2) - 4m_b^2 m_t^2 \right]; \quad (3.32)$$

$$\Gamma(t \rightarrow bW^+) = \frac{\sqrt{[m_t^2 - (m_W + m_b)^2][m_t^2 - (m_W - m_b)^2]}}{16\pi m_t^3} \cdot \mathcal{A}_W, \quad (3.33)$$

$$\mathcal{A}_W = \frac{g^2}{4m_W^2} \left[m_W^2(m_t^2 + m_b^2 - 2m_W^2) + (m_t^2 - m_b^2)^2 \right]. \quad (3.34)$$

With the help of fig. 2, which displays contours of $BR(t \rightarrow bW^+)$ in the (m_H, x) plane, we can see that deviations from the SM prediction $BR(t \rightarrow bW^+) \simeq 1$ can be very significant, up to $BR(t \rightarrow bW^+) \sim 0.4$. However, this requires some work to be transformed into a constraint on the parameter space, since the Tevatron experiments use to give their bounds on charged Higgs bosons [16] in terms of the parameters $(\tan \beta, m_H)$, as defined in a special subclass of two-doublet models, and in any case these bounds have some dependence on the assumed top production cross-section. As a tentative reference value for the CDF and D0 sensitivity, we can take $BR(t \rightarrow bW^+) = 0.6$. Even this conservative estimate is sufficient to rule out a significant region of the (m_H, x) plane, characterized by low values of m_H and x .

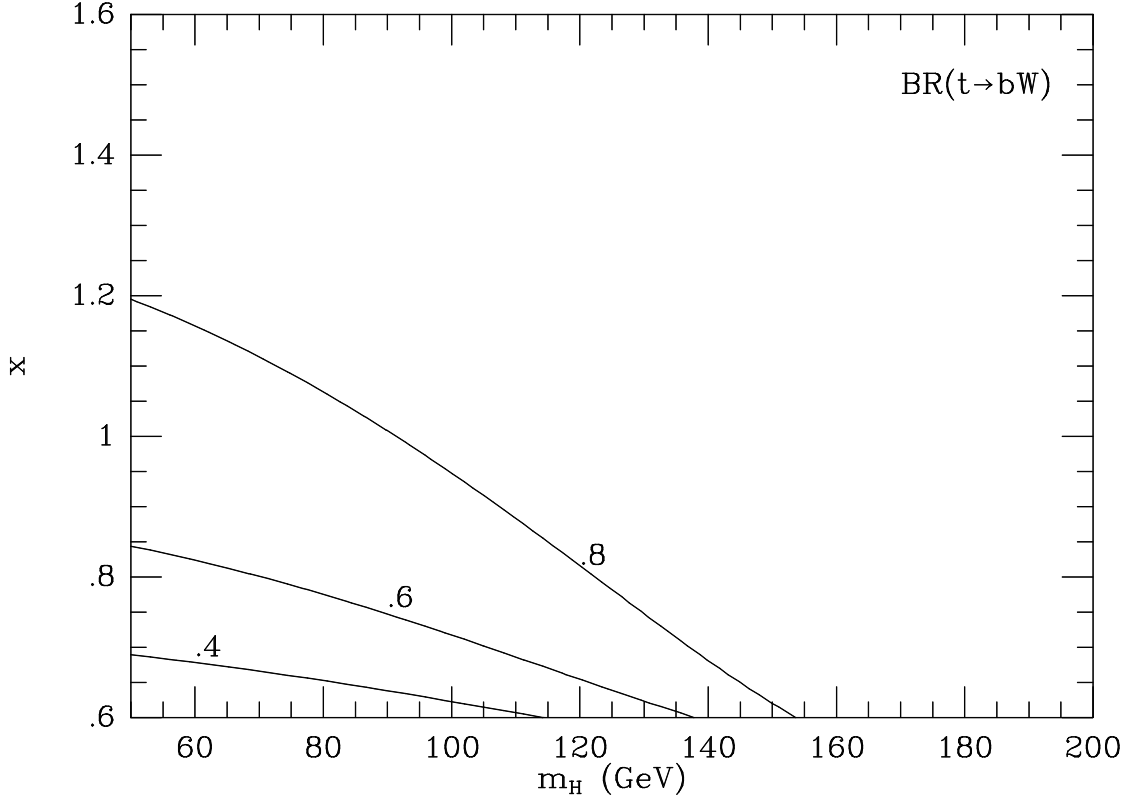


Figure 2: *Contours of $BR(t \rightarrow bW)$ in the (m_H, x) plane.*

3.4.1 $b \rightarrow s\gamma$

The experimental determination [17] of the inclusive $B \rightarrow X_s\gamma$ branching ratio, $BR(B \rightarrow X_s\gamma) = (2.32 \pm 0.67) \times 10^{-4}$, has been recently supplemented by the complete next-to-leading-order SM calculation [18], giving $BR(B \rightarrow X_s\gamma)_{SM} = (3.28 \pm 0.33) \times 10^{-4}$. These two results strongly constrain many possible extensions of the SM, and in particular the FP model, as we shall now see. Both in the SM and in the FP model, the dominant contribution comes from the effective operator $\mathcal{O}_7 \propto m_b \bar{s}_L \sigma^{\mu\nu} b_R F_{\mu\nu}$. Following the strategy of [13], we express our results in terms of the ratio

$$R_\gamma \equiv \frac{Br(B \rightarrow X_s\gamma)_{FP}}{Br(B \rightarrow X_s\gamma)_{SM}} \simeq \left[\frac{C(A_W + A_H)_{FP} + D}{C(A_W)_{SM} + D} \right]^2, \quad (3.35)$$

where $C \simeq 0.66$ and $D \simeq 0.35$ take into account the leading QCD corrections. In the SM, the dominant one-loop diagrams involve the exchange of virtual W bosons and top quarks, and give

$$(A_W)_{SM} = x_{tW} [2F_1(x_{tW}) + 3F_2(x_{tW})]. \quad (3.36)$$

Here and in the following, we set by convention $x_{ij} = m_i^2/m_j^2$. The explicit expression of the different F -functions can be found in the appendix of ref. [13]. In the FP model,

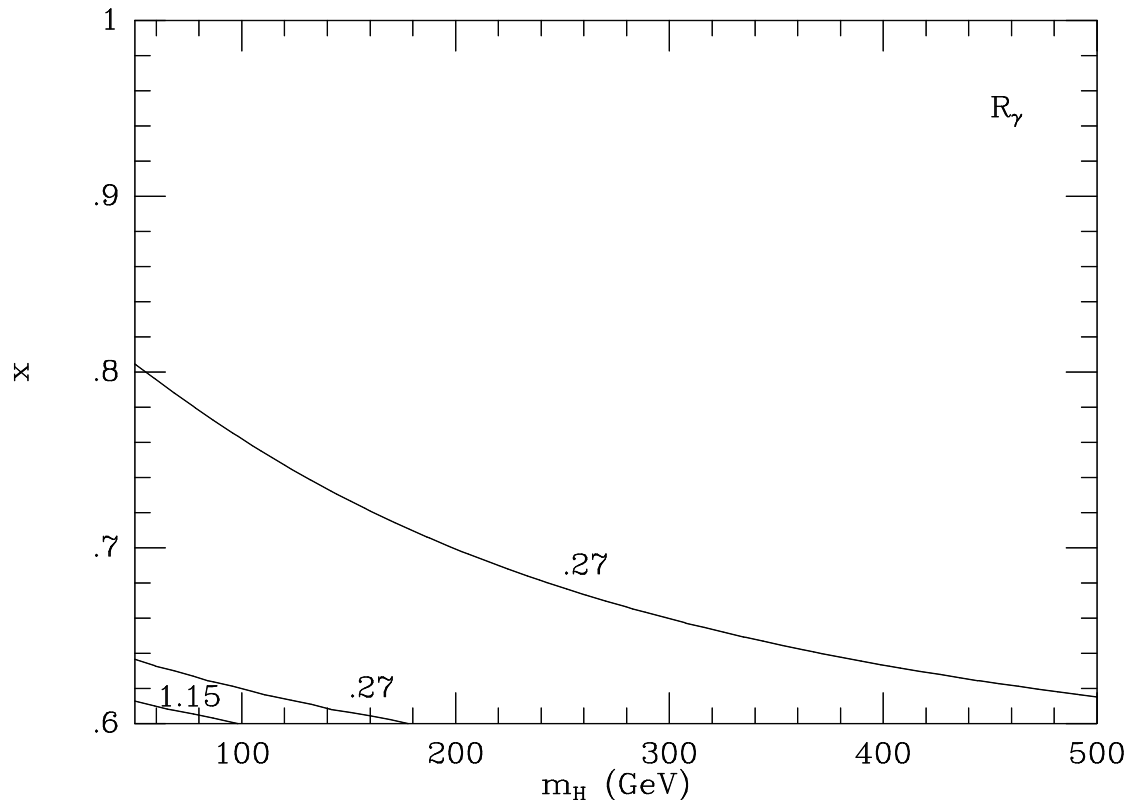


Figure 3: *Contours of R_γ in the (m_H, x) plane.*

considering the limit of vanishing mixing angle α_\pm , gauge boson exchange gives the same result as in the SM, eq. (3.36). One should add to the previous result the contributions from one-loop diagrams involving the exchange of virtual top quarks and charged Higgs bosons, which can be significant [19]. Working as before in the limiting case of eq. (2.50):

$$A_H^{FP} = \frac{x_{tH}}{3} \frac{t_W^2}{x^2 - t_W^2} [2F_1(x_{tH}) + 3F_2(x_{tH}) - 2F_3(x_{tH}) - 3F_4(x_{tH})] . \quad (3.37)$$

The possible values of R_γ in the (m_H, x) plane are shown by the contour plot of fig. 3. Our conservative estimate of the presently allowed range of variation is

$$0.27 < R_\gamma < 1.15 . \quad (3.38)$$

We then see that the constraint of eq. (3.38) excludes simultaneously small values of m_H and x , apart from a small strip near $x = 0.6$ and $m_H = 100$ GeV, which is however excluded by other constraints. Notice that, in contrast with other popular models, in the FP model a light charged Higgs is likely to give $R_\gamma < 1$.

3.4.2 $B_0 - \bar{B}_0$ and $K_0 - \bar{K}_0$ mixing

We discuss here the FP-model contributions to the $B_d^0 - \bar{B}_d^0$ mass difference Δm_{B_d} and to the CP-violation parameter of the $K^0 - \bar{K}^0$ system ϵ_K , and the constraints on the model parameters coming from the experimentally measured values of Δm_{B_d} and ϵ_K . As usual, we consistently neglect terms proportional to m_b in the charged Higgs vertices with top and bottom quarks.

For our purposes, a convenient way of parametrizing the $B_d^0 - \bar{B}_d^0$ mass difference is:

$$\Delta m_{B_d} = \eta_{B_d} \cdot \frac{4}{3} f_{B_d}^2 B_{B_d} \cdot m_{B_d} \cdot \left(\frac{\alpha_W}{4m_W} \right)^2 \cdot |K_{tb} K_{td}^*|^2 \cdot x_{tW} \cdot |\Delta|, \quad (3.39)$$

where $\eta_{B_d} \simeq 0.55$ is a QCD correction factor; f_{B_d} is the B_d decay constant and B_{B_d} the vacuum saturation parameter. The quantity Δ contains the dependence on the parameters of the FP model. We have checked that, for values of α_{\pm} and $m_{W'}$ allowed by other constraints, the contributions to Δ coming from box diagrams with internal W' lines can be safely neglected. We can then perform the following decomposition:

$$\Delta = \Delta_W + \Delta_H. \quad (3.40)$$

In eq. (3.40), Δ_W denotes the Standard Model contribution, associated with the box diagrams involving the top quark and the W boson:

$$\Delta_W = A(x_{tW}), \quad (3.41)$$

where the explicit expression of the function $A(x)$ can be found in the appendix of ref. [13]. Δ_H denotes the additional contributions from the box diagrams involving the physical charged Higgs bosons [20]. Working as before in the limiting case of eq. (2.50), we find:

$$\Delta_H = \lambda_H^4 x_{Wt} x_{WH} G(x_{tH}) + \lambda_H^2 [4F'(x_{tW}, x_{HW}) + G'(x_{tW}, x_{HW})], \quad (3.42)$$

where λ_H has been defined in eq. (3.28), and the functions $G(x)$, $F'(x, y)$ and $G'(x, y)$ are given in the appendix of ref. [13].

Moving to the $K^0 - \bar{K}^0$ system, the absolute value of the parameter ϵ_K is well approximated by the expression:

$$|\epsilon_K| = \frac{2}{3} f_K^2 B_K \cdot \frac{m_K}{\sqrt{2} \Delta m_K} \cdot \left(\frac{\alpha_W}{4m_W} \right)^2 \cdot x_{cW} \cdot |\Omega|, \quad (3.43)$$

where f_K is the K decay constant, B_K is the vacuum saturation parameter (recently re-evaluated in [21]), Δm_K is the experimental $K_L^0 - K_S^0$ mass difference. The quantity Ω , carrying the dependence on the mixing angles and the FP-model parameters, is given by:

$$\Omega = \eta_{cc} \text{Im}(K_{cs} K_{cd}^*)^2 + 2\eta_{ct} \text{Im}(K_{cs} K_{cd}^* K_{ts} K_{td}^*)^2 [B(x_{tW}) - \log x_{cW}] + \eta_{tt} \text{Im}(K_{ts} K_{td}^*)^2 x_{tc} \Delta, \quad (3.44)$$

where $\eta_{cc} \simeq 1.38$, $\eta_{ct} \simeq 0.47$ and $\eta_{tt} \simeq 0.57$ are QCD correction factors; $x_{cW} = m_c^2/m_W^2$, $x_{tc} = m_t^2/m_c^2$; the function $B(x)$ can be found in the appendix of ref. [13]; Δ is the same as in eq. (3.40). In principle, there are additional contributions due to charged Higgs exchange besides those appearing in Δ . However, in the FP model they can be safely neglected with respect either to the standard contribution or to the non-standard contribution parametrized by Δ , hence they have not been considered here.

We have studied the dependence of Δ on the parameters (m_H, x) , characterizing the charged Higgs sector. We observe that $\Delta_{FP} > \Delta_{SM}$. Some quantitative information is given in fig. 4, which displays contours of the ratio

$$R_\Delta \equiv \frac{\Delta}{\Delta_W} \quad (3.45)$$

in the plane (m_H, x) . Observe that values of R_Δ much larger than 1 can be obtained for small values of m_H and of x .

To discuss the constraints coming from the measured values of Δm_{B_d} and ϵ_K , we recall that the dependence on the FP-model parameters is contained in the quantity Δ of eq. (3.40), so it would be desirable to obtain from the experimental data a bound on Δ . On the other hand, this requires some knowledge of the parameters characterizing the mixing matrix K . Notice that we cannot rely upon the SM fit to the matrix K , since among the experimental quantities entering this fit there are precisely Δm_{B_d} and ϵ_K , whose description now differs from the SM one.

To derive the desired bound on Δ , we have used the results of the fit performed in [13]. As discussed there, it is not straightforward to translate those results into a single definite bound on Δ , or, equivalently, on $R_\Delta = \Delta/\Delta_W \simeq 1.8\Delta$. As a tentative bound we can consider here $0.4 < R_\Delta < 4$. Contours of R_Δ in the (m_H, x) plane are shown in fig. 4: we can see that small values of m_H and x are excluded.

3.5 W' and Z' signals at hadron colliders

In this section we analyse possible signals of the new vector bosons of the FP model at the Tevatron collider and at the LHC. We will obtain new restrictions on the parameter space of the FP model and describe some of its specific signatures. From the previous sections, we know that relatively light W' and Z' are not excluded, provided that x is sufficiently large. The neutral gauge boson Z' possesses a direct coupling to ordinary fermions that scales as $1/x$, and also an indirect coupling, via the mixing controlled by the angle α_0 , subject to the phenomenological restriction $|\alpha_0| \lesssim 10^{-2}$. On the other hand, the charged vector boson W' can couple to fermions only through the mixing controlled by the angle α_\pm , also subject to a similar phenomenological bound, $|\alpha_\pm| \lesssim 10^{-2}$.

Both Z' and W' can be produced at hadron colliders via quark-antiquark annihilation. In tables 7 and 8 we show the total cross-sections for the production of Z' and W' , respectively, at the Tevatron collider, $\sqrt{s} = 1.8$ TeV. The cross-sections have been evaluated in

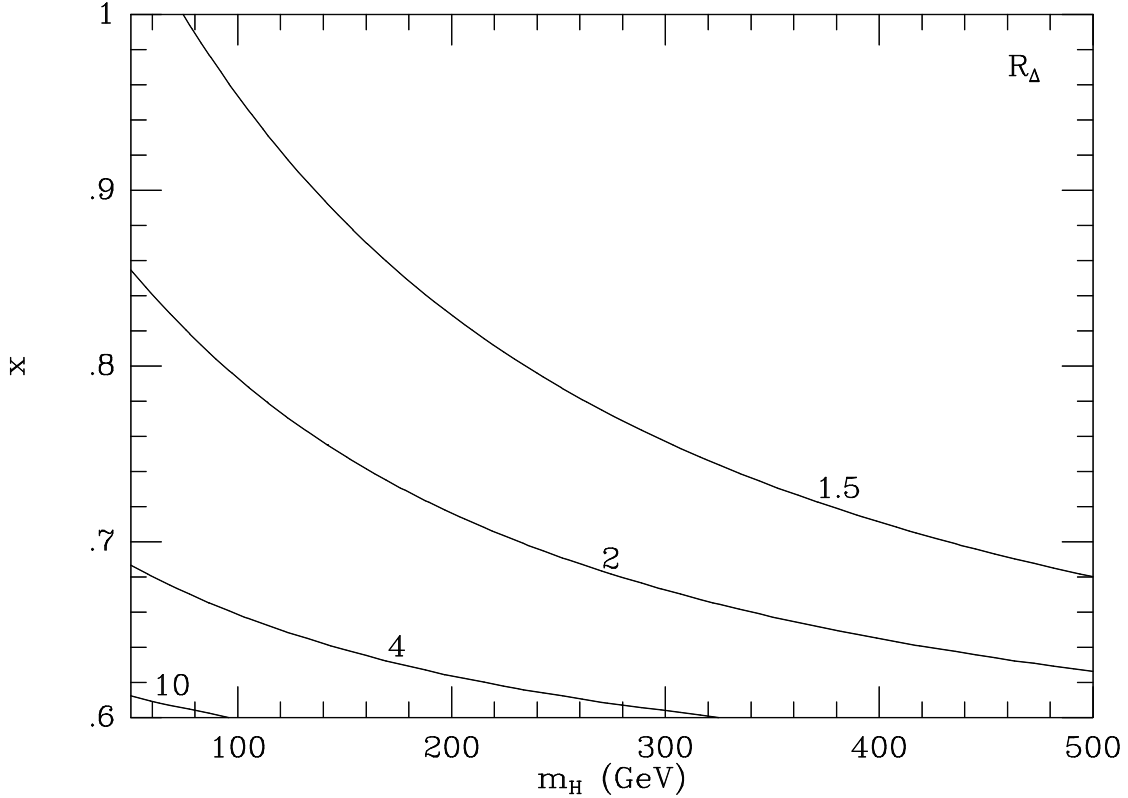


Figure 4: *Contours of R_Δ in the (m_H, x) plane.*

the narrow width approximation, using the parton densities of [22]. A K-factor $\simeq 1.2$ has been included.

The cross-sections of table 7 were computed in the limit $\alpha_0 = 0$. We checked that only small variations are induced by varying the mixing angle in the range $|\alpha_0| \leq 10^{-2}$. Indeed, we expect a dependence on α_0 only for large x , when the direct coupling and mixing effects become comparable. For $|\alpha_0| \sim 10^{-2}$, such a dependence would manifest approximately at $x \sim 10^2$, beyond the range explored here. Notice that the Z' cross section scales approximately as $1/x^2$, as expected from the x dependence of its couplings to fermions.

The W' cross-section scales as $(\alpha_\pm)^2$. Moreover, it is independent of x , since W' is coupled to the standard $SU(2)_L$ current. In table 8 we considered $\alpha_\pm = 0.01$, at the border of the region allowed by precision tests. Even in this case the W' cross-section is quite modest, below the observability level as soon as $m_{W'}$ is larger than 250 GeV. The big difference between the Z' and W' cross-sections listed in tables 7 and 8 is largely due to the different interaction properties of Z' and W' with fermions. Due to the suppression of W' production at hadron colliders, the only significant limitations on the parameter space from the Tevatron data are those that can be obtained through the study of the Z' channel.

$m_{Z'}$ (GeV)	$x = 0.6$	$x = 1$	$x = 5$	$x = 20$
100	$1.4 \cdot 10^4$	$12.5 \cdot 10^2$	35.4	2.2
250	$8.1 \cdot 10^2$	71.0	2.0	$12.5 \cdot 10^{-2}$
500	41.2	3.6	$10.2 \cdot 10^{-2}$	$63.2 \cdot 10^{-4}$
1000	$9.3 \cdot 10^{-2}$	$81.0 \cdot 10^{-4}$	$2.3 \cdot 10^{-4}$	$14.2 \cdot 10^{-6}$

Table 7: *Total cross-section in pb for Z' production at the Tevatron collider, $\sqrt{s} = 1.8$ TeV for $\alpha_0 = 0$.*

$m_{W'}$ (GeV)	100	250	500	1000
$\sigma_{W'}(pb)$	0.6	$2.8 \cdot 10^{-2}$	$9.8 \cdot 10^{-4}$	$1.3 \cdot 10^{-6}$

Table 8: *Total cross-section in pb for W' production at the Tevatron collider, $\sqrt{s} = 1.8$ TeV for $\alpha_{\pm} = 10^{-2}$.*

In the range of parameters considered in table 7, the Z' cross-section at the Tevatron collider is sizeable and might have produced an observable signal. Beyond the traditional dilepton channel [23], the CDF and D0 collaborations have recently searched for Z' in the dijet and in the $b\bar{b}$ channels [24]. Moreover, the same collaborations have measured the cross-sections for diboson production [25], which can be modified in the presence of a Z' . Indeed, the Z' of the FP model can decay into fermion-antifermion pairs, or in WW , WW' , $W'W'$ and Zh , when kinematically possible.

In the limit of vanishing mixing angles α_0 and α_{\pm} , the tree-level interaction terms $Z'WW$, $Z'WW'$, $Z'Zh$ vanish together with the corresponding Z' partial widths. In this approximation Z' decays almost exclusively in leptons or quark pairs, in the ratios 15:3:5:17 for (massless) e^+e^- , $\nu\bar{\nu}$, $u\bar{u}$ and $d\bar{d}$, respectively. On the experimental side, the sensitivity is larger for the dilepton channel (e^+e^- and $\mu^+\mu^-$) than for the dijet or $b\bar{b}$ channels. The dilepton search provides the most stringent constraint on the FP model.

For non-vanishing mixing angles, the branching ratios of Z' into WW and Zh can become comparable with those into fermions. For instance, it is well known [26] that in the WW channel the suppression α_0^2 in the squared coupling constant can be compensated by the kinematical factor $(m_{Z'}/m_W)^4$, for sufficiently large $m_{Z'}$. Moreover, the fermionic modes can be depleted by a large x value.

In fig. 5 we show some of the Z' branching ratios, as functions of x , for $m_{Z'} = 400, 1000$ GeV, $\alpha_0 = \alpha_{\pm} = 0.01$ and $m_h = 200$ GeV: the line denoted by ll corresponds to decays into charged lepton pairs of a single generation, the one denoted by qq to decays into all possible quark-antiquark pairs; the branching ratio for the decays into neutrino pairs is not shown. When x is close to its lower bound, the fermionic channels are en-

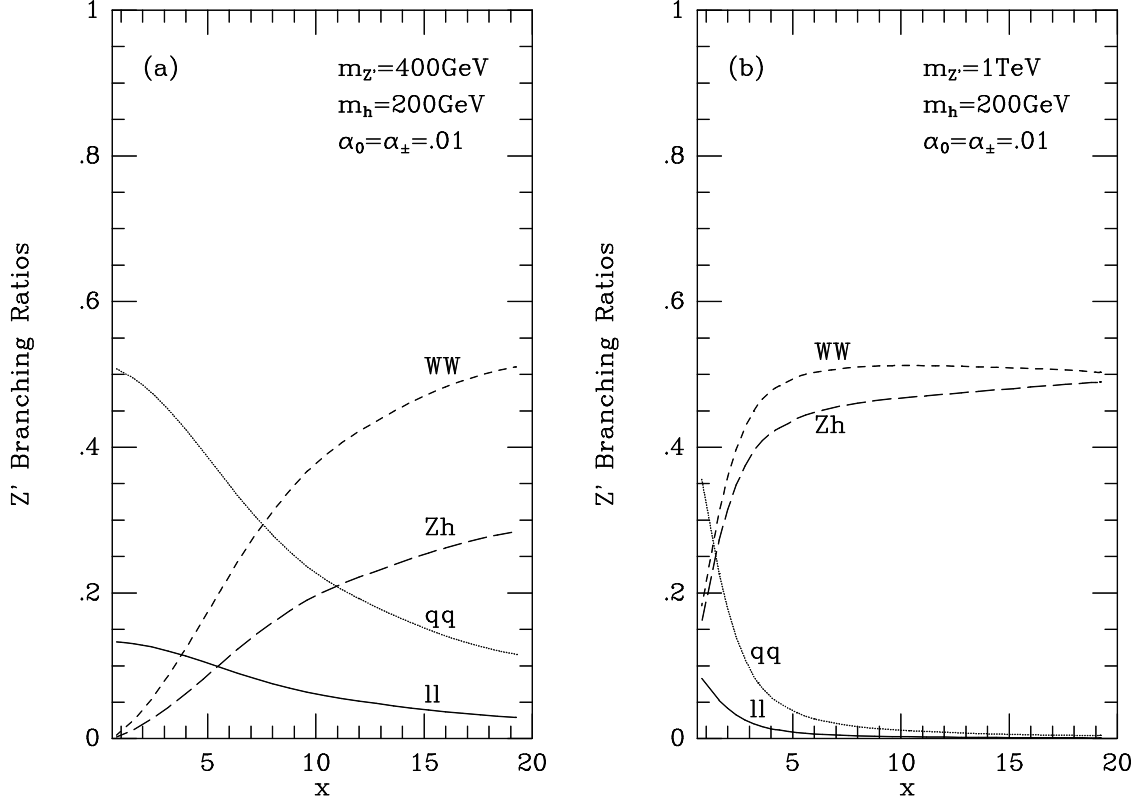


Figure 5: Z' branching ratios, as functions of x , for $m_h = 200$ GeV, $\alpha_0 = \alpha_{\pm} = 0.01$ and: (a) $m_{Z'} = 400$ GeV; (b) $m_{Z'} = 1$ TeV.

hanced due to the large coupling constant. Moving to larger values of x , the fermionic branching ratios decrease. When $m_{Z'} = 400$ GeV, they are reduced by a factor 5 going from $x = 0.6$ to $x = 20$. When $m_{Z'} = 1000$ GeV, the reduction factor is about 160 in the same x interval. The larger suppression for larger values of $m_{Z'}$ is due to the positive powers of $(m_{Z'}/m_Z)$ that characterize the diboson channels. Moreover, when $m_{Z'}$ is large, smaller values of x are needed to obtain significant branching ratios into WW or Zh .

In practice, however, for those values of $m_{Z'}$ and x that make the diboson channels dominant, the total cross-section for Z' production becomes small. We have explicitly verified that the most stringent bound from the Tevatron is always the one related to dilepton searches.

The total Z' width, $\Gamma_{Z'}$, strongly depends on x . When x is close to its lower bound, $\Gamma_{Z'}/m_{Z'}$ is dominated by the fermionic channels. For $x = 0.6$, $\Gamma_{Z'}/m_{Z'}$ ranges between 0.07 and 0.085 for $m_{Z'}$ in the interval (100, 1000) GeV. For large x values, the width is saturated by the WW and Zh channels, and $\Gamma_{Z'}/m_{Z'}$ never exceeds few per mille for $m_{Z'} < 1$ TeV.

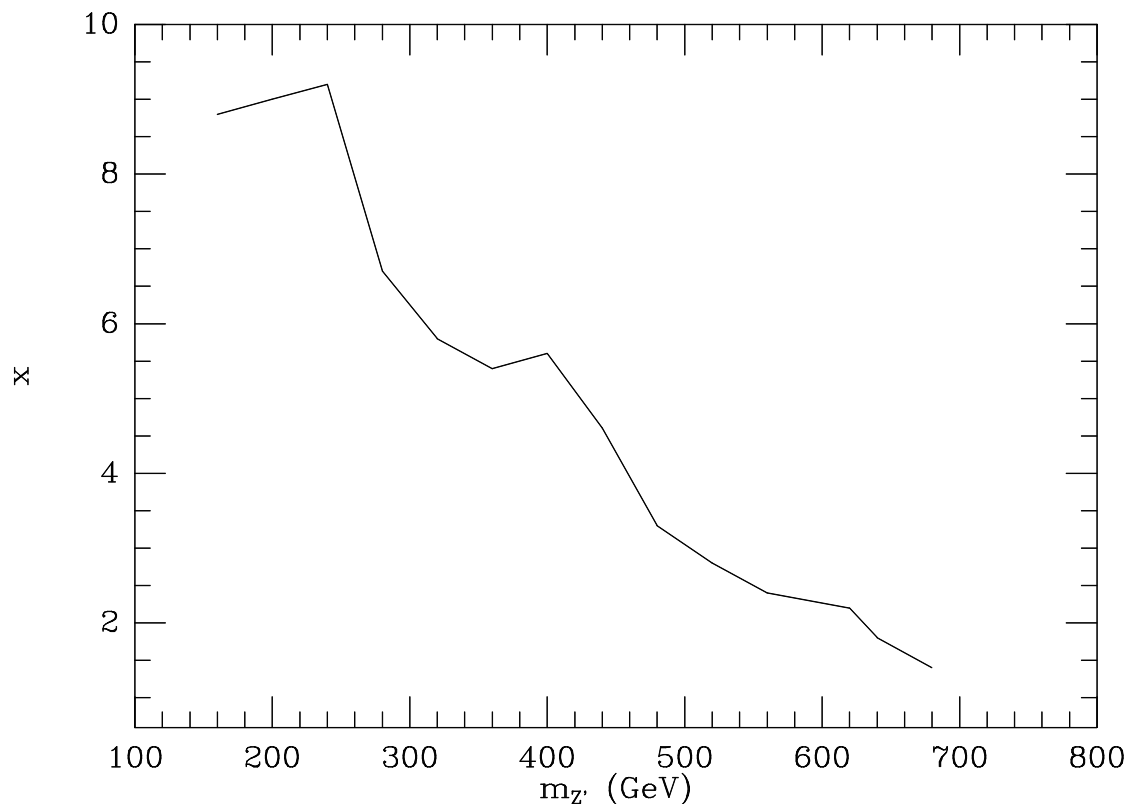


Figure 6: *Region of the $(m_{Z'}, x)$ plane excluded by dilepton searches at the Tevatron collider.*

In fig. 6 we present the region of the $(m_{Z'}, x)$ plane excluded by dilepton searches⁵ at $\sqrt{s} = 1.8$ TeV. We have considered the case $\alpha_0 = 0$. By turning α_0 on, the leptonic branching ratio is modified only in extreme regions of the $(m_{Z'}, x)$ plane. We checked that the exclusion region of fig. 6 is not sensitive to (small) non-zero values of α_0 . When $x = 1$, a lower bound on $m_{Z'}$ of approximately 670 GeV is obtained, numerically close to the lower bound on a Z' with SM couplings. On the other hand, for larger x lighter Z' are still allowed by the Tevatron data. For instance, $m_{Z'} = 300$ GeV is permitted when $x > 6$.

We conclude our discussion about the Tevatron data by adding some comments on the special configuration $v_1 = v_2 = v$ and $v_R = v_L/x$, selected in section 3.3.1 by the analysis of the one-loop scalar contribution to the ρ parameter. We have seen that in this case quite large values of x are required to obtain a reasonable fit of the electroweak data. The properties of W' and Z' are now similar. They are degenerate in mass. The mixing angles α_0 and α_{\pm} scale as $1/x$. Direct coupling and mixing effects are comparable for Z' , and both are suppressed by a $1/x$ factor. The branching ratios of Z' and W' are now

⁵In view of the difficulty of combining the CDF and D0 data [23], we have tentatively taken a rough interpolation of the CDF exclusion contour in the $(m_{Z'}, \sigma \cdot BR(Z' \rightarrow \bar{l}l))$ plane.

$m_{Z'} \text{ (GeV)}$	$x=0.6$	$x=1$	$x=5$	$x=20$
500	$6.69 \cdot 10^2$	58.5	1.66	0.10
1000	52.8	4.62	0.13	$0.8 \cdot 10^{-2}$
2500	0.66	0.06	$0.2 \cdot 10^{-2}$	$1 \cdot 10^{-4}$
5000	$0.3 \cdot 10^{-2}$	$2 \cdot 10^{-4}$	$7 \cdot 10^{-6}$	$4 \cdot 10^{-7}$

Table 9: *Total Z' cross-section, in pb, at the LHC, $\sqrt{s} = 14$ TeV, for $\alpha_0 = 0$.*

dominated by the fermionic channels. In particular the Z' branching ratio into electrons and muons is about 9%. For $x \gtrsim 20$ the whole mass range $m_{Z'} > 400$ GeV is allowed by the Tevatron data.

Finally, we have looked for possible signals of the FP model at the LHC. In table 9 we show the total cross-section for Z' production at a pp collider with $\sqrt{s} = 14$ TeV. As for the Tevatron collider, we find only modest variations of the cross-section when varying the mixing angle α_0 in the range allowed by the present bounds. Assuming an integrated luminosity of 10^5 pb^{-1} , from table 9 we can see that, at least in principle, even a Z' with $m_{Z'} = 5$ TeV is within the reach of the LHC, as long as $x < 1$.

We should however pay attention to the Z' branching ratios, which could vary substantially moving in the allowed parameter space. On one side, for very large values of $m_{Z'}$ such as those potentially interesting for the LHC, the WW width benefits from the huge enhancement factor $(m_{Z'}/m_W)^4$. On the other hand, for fixed values of x , $m_{Z'}$ and α_{\pm} , not all values of the mixing angle α_0 are allowed⁶. For instance, assuming $\alpha_{\pm} = 0$, the structure of the neutral gauge boson mass matrix gives rise to the following bound on α_0 :

$$-\frac{y^2 \sqrt{x^2 + y^2 + x^2 y^2}}{x^2 + y^2} \frac{m_W^2}{(m_{Z'}^2 - m_Z^2)} \leq s_0 c_0 \leq \frac{x^2 \sqrt{x^2 + y^2 + x^2 y^2}}{x^2 + y^2} \frac{m_W^2}{(m_{Z'}^2 - m_Z^2)}, \quad (3.46)$$

as can be easily checked by diagonalizing it exactly. For instance, a mixing angle $\alpha_0 = 0.01$, allowed by the precision tests, is incompatible with the simultaneous choices $x = 0.6$ and $m_{Z'} = 5$ TeV. Since the bounds in eq. (3.46) scale approximately as $m_W^2/m_{Z'}^2$, for large $m_{Z'}$, the enhancement factor is totally reabsorbed by the factor $(\alpha_0)^2$, and $\Gamma(Z' \rightarrow WW)/m_{Z'}$ cannot grow arbitrarily. A similar behaviour holds for the partial width $\Gamma(Z' \rightarrow Zh)$, which, for asymptotically large $m_{Z'}$ values, coincides with $\Gamma(Z' \rightarrow WW)$.

A first, rough estimate of the LHC discovery reach can be obtained by requiring at least 10 events in the e^+e^- or $\mu^+\mu^-$ channels for an integrated luminosity of 10^5 pb^{-1} , neglecting cuts, efficiencies, any detail of the experimental apparatus and considering the case of vanishing mixing angles, $\alpha_0 = \alpha_{\pm} = 0$, for which the only decay channels are the fermionic ones. In fig. 7 we exhibit the region which could be probed by the LHC on the basis of this simple criterium. The plot closer to the origin is the exclusion region from the Tevatron, presented here for comparison.

⁶For a discussion of the same phenomenon in a different context, see [26].

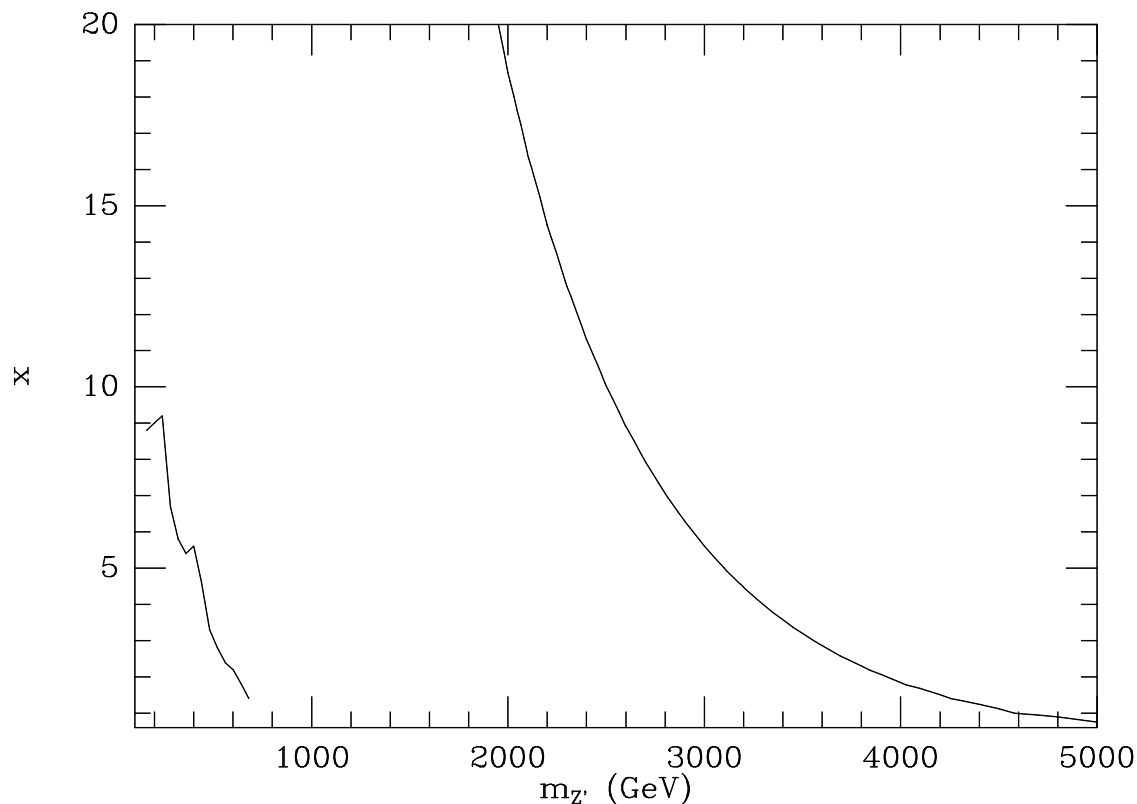


Figure 7: *Region of the $(m_{Z'}, x)$ plane accessible via dilepton searches at the LHC.*

It should be stressed that, when a non vanishing mixing angle α_0 is considered, the discovery region of fig. 7 may become smaller, due to the reduced dilepton branching ratio. Assuming for simplicity a vanishing mixing in the charged sector, the angle α_0 can vary in the range defined by eq. (3.46) and, depending on the actual values of $(x, m_{Z'})$, the diboson channel may compete with the dilepton one. For large $m_{Z'}$ and small x , the diboson branching ratios are negligible compared to the leptonic one. For instance, taking $m_{Z'} = 5000$ GeV and $x = 0.6$, the fermionic branching fractions are essentially constant in all the allowed α_0 range. Indeed, as can be deduced by eq. (3.46), such a range becomes quite narrow for small x and large $m_{Z'}$, and one approaches the case of vanishing α , where the diboson channels are absent.

On the contrary, moving to the region of larger x and smaller $m_{Z'}$, i.e. climbing up the curve of fig. 7, the fermionic Z' couplings decrease and the permitted α_0 interval becomes wider, allowing for conspicuous diboson branching ratios. For instance, on the points that correspond to $m_{Z'} = (4, 3, 2)$ TeV along the LHC contour, we find that the dilepton branching ratio can be as small as $(6 \cdot 10^{-2}, 1 \cdot 10^{-3}, 1 \cdot 10^{-4})$, respectively, clearly reducing the discovery potential of the LHC in the combined $(e^+e^-, \mu^+\mu^-)$ channel. On the other hand, for the same $m_{Z'}$ values, the WW and Zh branching ratios are approximately the same (for light h) and are given by $(.38, .50, .50)$, respectively. This opens the possibility

of compensating the reduced sensitivity to charged leptons with a dedicated search in the diboson channels. In particular, the Zh mode, followed by the decay of Z into l^+l^- ($l = e, \mu$) and by the decay of h into $b\bar{b}$ may provide an interesting signature of the model. The study of the corresponding discovery reach at the LHC requires however knowledge of acceptances and efficiencies of the experimental apparatus as well as a study of the relevant backgrounds within appropriate kinematical cuts, which goes beyond the scope of this work.

In conclusion, we have analysed an anomaly-free $SU(2)_R$ extension of the SM, with no tree-level FCNC. The $SU(2)_R$ gauge bosons and the scalars in the ϕ_R, ϕ_{LR} multiplets have no coupling with the ordinary fermions. Tree-level effects are dominated by a new neutral gauge boson Z' that mainly couples to the hypercharge. A comparison with the available electroweak data severely constrains the mixing angles, both in the neutral and in the charged gauge boson sector, still allowing for a region of parameter space with relatively light new gauge vector bosons. Loop effects may instead be dominated by Higgs exchange. We have discussed several possibilities to cancel the 1-loop contribution to the ρ parameter quadratic in the scalar masses. The remaining loop effects are mainly due to charged Higgs exchange and are constrained by data on FCNC processes and by R_b . This last constraint is the most restrictive one, and limits the possible values of the charged Higgs masses and of the g_R coupling. Differently from the usual LR extension of the SM, the W' contribution to FCNC effects is negligible, thanks to the strict limits on the α_{\pm} angle and to the fermiophobic nature of W' . Also the direct search for a Z' in the dilepton channel at the Tevatron collider leads to an excluded region in the $(m_{Z'}, g_R)$ plane, which however does not prevent the possibility of relatively light new vector bosons, if g_R is sufficiently large. Only the LHC collider will have sufficient sensitivity to test new W' and Z' in the TeV range.

Acknowledgements

We would like to thank G. Chiarelli for useful discussions. One of us (J.M.) acknowledges financial support from Ministerio de Educación y Ciencia (Spain).

Appendix A

We collect here some details of the spectrum and interactions in the FP model.

The explicit form of the orthogonal 4×4 matrix A , connecting mass and interaction eigenstates in the charged Higgs sector and defined by eq. (2.29), is

$$A = \begin{pmatrix} \frac{xv_R}{N_1}t_\alpha & \frac{xv_R}{N_2} & e_1^{(1)} & e_1^{(2)} \\ \frac{v_L}{N_1} & -\frac{v_L}{N_2}t_\alpha & e_2^{(1)} & e_2^{(2)} \\ \frac{v_1 - v_2xt_\alpha}{N_1} & -\frac{v_1t_\alpha + v_2x}{N_2} & e_3^{(1)} & e_3^{(2)} \\ \frac{v_1xt_\alpha - v_2}{N_1} & \frac{v_1x + t_\alpha v_2}{N_2} & e_4^{(1)} & e_4^{(2)} \end{pmatrix}, \quad (\text{A.1})$$

where

$$e^{(1)} = v_L v_R \left(\left[\frac{v_2 c_\beta}{v_R N_3} - \frac{(v_2 a - v_1) s_\beta}{v_R N_4} \right], \left[\frac{-v_1 c_\beta}{v_L N_3} + \frac{(v_1 a - v_2) s_\beta}{v_L N_4} \right], \left[\frac{c_\beta}{N_3} - \frac{a s_\beta}{N_4} \right], -\frac{s_\beta}{N_4} \right)^T$$

$$e^{(2)} = v_L v_R \left(\left[\frac{v_2 s_\beta}{v_R N_3} + \frac{(v_2 a - v_1) c_\beta}{v_R N_4} \right], \left[\frac{-v_1 s_\beta}{v_L N_3} - \frac{(v_1 a - v_2) c_\beta}{v_L N_4} \right], \left[\frac{s_\beta}{N_3} + \frac{a c_\beta}{N_4} \right], \frac{c_\beta}{N_4} \right)^T.$$

In the above equation, we should understand $s_{\alpha(\beta)} \equiv \sin \alpha_\pm(\beta_\pm)$, $c_{\alpha(\beta)} \equiv \cos \alpha_\pm(\beta_\pm)$, $t_{\alpha(\beta)} \equiv \tan \alpha_\pm(\beta_\pm)$ and, with the same conventions:

$$a = \frac{v_1 v_2 (v_L^2 + v_R^2)}{v_R^2 v_L^2 + v_1^2 v_R^2 + v_2^2 v_L^2}, \quad (\text{A.2})$$

$$N_1^2 = v_L^2 + u^2 + x^2 (v_R^2 + u^2) t_\alpha^2 - 4v_1 v_2 x t_\alpha, \quad (\text{A.3})$$

$$N_2^2 = (v_L^2 + u^2) t_\alpha^2 + x^2 (v_R^2 + u^2) + 4v_1 v_2 x t_\alpha, \quad (\text{A.4})$$

$$N_3^2 = v_R^2 v_L^2 + v_1^2 v_R^2 + v_2^2 v_L^2, \quad (\text{A.5})$$

$$N_4^2 = N_3^2 \left(\frac{v_L^2 v_R^2 + v_1^2 v_L^2 + v_2^2 v_R^2}{v_L^2 v_R^2 + v_2^2 v_L^2 + v_1^2 v_R^2} - a^2 \right). \quad (\text{A.6})$$

The explicit form of the orthogonal 4×4 matrix C , connecting mass and interaction eigenstates in the neutral CP-odd Higgs sector and defined by eq. (2.30), is

$$C = \begin{pmatrix} \frac{(x^2 + y^2)v_R}{M_1}t_\alpha & \frac{(x^2 + y^2)v_R}{M_2} & d_1^{(1)} & d_1^{(2)} \\ \frac{s_W y^2 t_\alpha + xy}{s_W M_1} v_L & \frac{s_W y^2 - xy t_\alpha}{s_W M_2} v_L & d_2^{(1)} & d_2^{(2)} \\ \frac{-s_W x^2 t_\alpha + xy}{s_W M_1} v_1 & \frac{-s_W x^2 - xy t_\alpha}{s_W M_2} v_1 & d_3^{(1)} & d_3^{(2)} \\ \frac{s_W x^2 t_\alpha - xy}{s_W M_1} v_2 & \frac{s_W x^2 + xy t_\alpha}{s_W M_2} v_2 & d_4^{(1)} & d_4^{(2)} \end{pmatrix}, \quad (\text{A.7})$$

where

$$d^{(1)} = v_L v_R \left(\left[\frac{v_1 c_\beta}{v_R M_3} - \frac{(v_1 b - v_2) s_\beta}{v_R M_4} \right], \left[\frac{-v_1 c_\beta}{v_L M_3} + \frac{(v_1 b - v_2) s_\beta}{v_L M_4} \right], \left[\frac{c_\beta}{M_3} - \frac{b s_\beta}{M_4} \right], -\frac{s_\beta}{M_4} \right)^T$$

$$d^{(2)} = v_L v_R \left(\left[\frac{v_1 s_\beta}{v_R M_3} + \frac{(v_1 b - v_2) c_\beta}{v_R M_4} \right], \left[\frac{-v_1 s_\beta}{v_L M_3} - \frac{(v_1 b - v_2) c_\beta}{v_L M_4} \right], \left[\frac{s_\beta}{M_3} + \frac{b c_\beta}{M_4} \right], \frac{c_\beta}{M_4} \right)^T$$

In the above equation, we should understand $s_{\alpha(\beta)} \equiv \sin \alpha_0(\beta_0)$, $c_{\alpha(\beta)} \equiv \cos \alpha_0(\beta_0)$, $t_{\alpha(\beta)} \equiv \tan \alpha_0(\beta_0)$ and, with the same conventions:

$$b = \frac{v_1 v_2 (v_L^2 + v_R^2)}{v_L^2 v_R^2 + v_1^2 (v_L^2 + v_R^2)}, \quad (\text{A.8})$$

$$M_1^2 = (v_L^2 + u^2)(x^2 + y^2 + x^2 y^2) + (v_R^2 (x^2 + y^2)^2 + u^2 x^4 + v_L^2 y^4) t_\alpha^2 - 2(x^2 u^2 - y^2 v_L^2) t_\alpha \sqrt{x^2 + y^2 + x^2 y^2}, \quad (\text{A.9})$$

$$M_2^2 = (v_L^2 + u^2)(x^2 + y^2 + x^2 y^2) t_\alpha^2 + (v_R^2 (x^2 + y^2)^2 + u^2 x^4 + v_L^2 y^4) + 2(x^2 u^2 - y^2 v_L^2) t_\alpha \sqrt{x^2 + y^2 + x^2 y^2}, \quad (\text{A.10})$$

$$M_3^2 = v_L^2 v_R^2 + v_1^2 (v_R^2 + v_L^2), \quad (\text{A.11})$$

$$M_4^2 = M_3^2 \left(\frac{v_L^2 v_R^2 + v_2^2 (v_R^2 + v_L^2)}{v_L^2 v_R^2 + v_1^2 (v_R^2 + v_L^2)} - b^2 \right). \quad (\text{A.12})$$

In terms of the mass eigenstates in the gauge boson sector, (W, W') and (A, Z, Z') , the trilinear gauge boson vertices read:

$$\begin{aligned} & + ig \left(c_W c_0 c_\pm^2 + \frac{x^2}{\sqrt{x^2 + y^2}} s_0 s_\pm^2 - \frac{x^2 y^2}{\sqrt{x^2 + y^2} \sqrt{x^2 + y^2 + x^2 y^2}} c_0 s_\pm^2 \right) \times \\ & \quad (W_\nu^- \partial_\mu W_\nu^+ Z_\mu + W_\mu^+ \partial_\mu W_\nu^- Z_\nu + W_\mu^- W_\nu^+ \partial_\mu Z_\nu) \\ & + ig \left(c_W c_0 s_\pm^2 + \frac{x^2}{\sqrt{x^2 + y^2}} s_0 c_\pm^2 - \frac{x^2 y^2}{\sqrt{x^2 + y^2} \sqrt{x^2 + y^2 + x^2 y^2}} c_0 c_\pm^2 \right) \times \\ & \quad (W_\nu'^- \partial_\mu W_\nu'^+ Z_\mu + W_\mu'^+ \partial_\mu W_\nu'^- Z_\nu + W_\mu'^- W_\nu'^+ \partial_\mu Z_\nu) \\ & + ig \left(-c_W s_0 c_\pm^2 + \frac{x^2}{\sqrt{x^2 + y^2}} c_0 s_\pm^2 + \frac{x^2 y^2}{\sqrt{x^2 + y^2} \sqrt{x^2 + y^2 + x^2 y^2}} s_0 s_\pm^2 \right) \times \\ & \quad (W_\nu^- \partial_\mu W_\nu^+ Z'_\mu + W_\mu^+ \partial_\mu W_\nu^- Z'_\nu + W_\mu^- W_\nu^+ \partial_\mu Z'_\nu) \\ & - ig c_\pm s_\pm \left(c_W c_0 - \frac{x^2}{\sqrt{x^2 + y^2}} s_0 + \frac{x^2 y^2}{\sqrt{x^2 + y^2} \sqrt{x^2 + y^2 + x^2 y^2}} c_0 \right) \times \\ & \quad (W_\nu'^- \partial_\mu W_\nu'^+ Z_\mu + W_\mu'^+ \partial_\mu W_\nu'^- Z_\nu + W_\mu'^- W_\nu'^+ \partial_\mu Z_\nu + \\ & \quad W_\nu^- \partial_\mu W_\nu'^+ Z_\mu + W_\mu^+ \partial_\mu W_\nu'^- Z_\nu + W_\nu'^+ W_\mu^- \partial_\mu Z_\nu) \\ & - ig c_\pm s_\pm \left(-c_W s_0 - \frac{x^2}{\sqrt{x^2 + y^2}} c_0 - \frac{x^2 y^2}{\sqrt{x^2 + y^2} \sqrt{x^2 + y^2 + x^2 y^2}} s_0 \right) \times \\ & \quad (W_\nu'^- \partial_\mu W_\nu'^+ Z'_\mu + W_\mu'^+ \partial_\mu W_\nu'^- Z'_\nu + W_\mu'^- W_\nu'^+ \partial_\mu Z'_\nu + \\ & \quad W_\nu^- \partial_\mu W_\nu'^+ Z'_\mu + W_\mu^+ \partial_\mu W_\nu'^- Z'_\nu + W_\nu'^+ W_\mu^- \partial_\mu Z'_\nu) \\ & + ig \left(-c_W s_0 s_\pm^2 + \frac{x^2}{\sqrt{x^2 + y^2}} c_0 c_\pm^2 + \frac{x^2 y^2}{\sqrt{x^2 + y^2} \sqrt{x^2 + y^2 + x^2 y^2}} s_0 c_\pm^2 \right) \times \\ & \quad (W_\nu'^- \partial_\mu W_\nu'^+ Z'_\mu + W_\mu'^+ \partial_\mu W_\nu'^- Z'_\nu + W_\mu'^- W_\nu'^+ \partial_\mu Z'_\nu) \\ & + ig s_W (A_\mu W_\nu^- \partial_\mu W_\nu^+ + A_\nu W_\mu^+ \partial_\mu W_\nu^- + W_\mu^- W_\nu^+ \partial_\mu A_\nu) \end{aligned}$$

$$+igs_W \left(A_\mu W_\nu'^- \partial_\mu W_\nu'^+ + A_\nu W_\mu'^+ \partial_\mu W_\nu'^- + W_\mu'^- W_\nu'^+ \partial_\mu A_\nu \right). \quad (\text{A.13})$$

It is understood that we should add to the previous couplings their hermitean conjugates, and we have used the conventions $s_\pm \equiv \sin \alpha_\pm$, $c_\pm \equiv \cos \alpha_\pm$, $s_0 \equiv \sin \alpha_0$, $c_0 \equiv \cos \alpha_0$, $s_W \equiv \sin \theta_W$, $c_W \equiv \cos \theta_W$.

The cubic bosonic couplings involving the SM-like Higgs h , defined by eq. (2.32), and the gauge boson mass eigenstates are, in the same conventions as before:

$$\begin{aligned} & - \frac{1}{\sqrt{v_L^2 + v_1^2 + v_2^2}} \frac{h}{2} g_R^2 v_R^2 s_\pm c_\pm (W_\mu^- W'^{\mu+} + W_\mu^+ W'^{\mu-}) \\ & + \frac{1}{\sqrt{v_L^2 + v_1^2 + v_2^2}} h (2m_W^2 - \frac{1}{2} g_R^2 v_R^2 s_\pm^2) W_\mu^- W'^{\mu+} \\ & + \frac{1}{\sqrt{v_L^2 + v_1^2 + v_2^2}} h (2m_W'^2 - \frac{1}{2} g_R^2 v_R^2 c_\pm^2) W_\mu'^- W'^{\mu+} \\ & - \frac{1}{\sqrt{v_L^2 + v_1^2 + v_2^2}} \frac{h}{2} (g_R^2 + \tilde{g}^2) v_R^2 s_0 c_0 Z_\mu Z'^\mu \\ & + \frac{1}{\sqrt{v_L^2 + v_1^2 + v_2^2}} \frac{h}{2} (2m_Z^2 - \frac{1}{2} (g_R^2 + \tilde{g}^2) v_R^2 s_0^2) Z_\mu Z'^\mu \\ & + \frac{1}{\sqrt{v_L^2 + v_1^2 + v_2^2}} \frac{h}{2} (2m_Z'^2 - \frac{1}{2} (g_R^2 + \tilde{g}^2) v_R^2 c_0^2) Z'_\mu Z'^\mu. \end{aligned} \quad (\text{A.14})$$

Appendix B

We collect in this appendix the explicit expressions, valid at the classical level, for the most important partial decay rates of the W' and Z' bosons in the FP model.

From the explicit expressions of the charged currents, given in section 2.2.1, we can easily derive the vector and axial couplings of fermion doublets $f \equiv \{f_1, f_2\}$ to the charged vector boson W' :

$$v_f(W') = a_f(W') = -s_\pm a_f(W_L) \frac{g}{\sqrt{2}} T_L(f_L). \quad (\text{B.1})$$

The partial decay rates of W' into fermion pairs are then given by the standard formulae:

$$\Gamma(W' \rightarrow f_1 \bar{f}_2) = C_f |K_{f_1 f_2}|^2 \frac{m_{W'}}{12\pi} [1 - 2(x'_1 + x'_2) + (x'_1 - x'_2)^2]^{1/2} \quad (\text{B.2})$$

$$\left\{ [v_f^2(W') + a_f^2(W')] \left[1 - \frac{x'_1 + x'_2}{2} - \frac{(x'_1 - x'_2)^2}{2} \right] + 3 [v_f^2(W') - a_f^2(W')] (x'_1 x'_2)^{1/2} \right\}, \quad (\text{B.3})$$

where $C_f = 1, 3$ is the colour factor, $x'_{1,2} \equiv m_{f_{1,2}}^2/m_{W'}^2$ and K is the CKM matrix.

From the explicit expressions of the neutral currents, given in section 2.2.1, we can easily derive the vector and axial couplings of fermions to the neutral vector boson Z' :

$$\begin{aligned} v_f(Z_L) &= \frac{e}{s_W c_W} \left[\frac{T_{3L}(f_L)}{2} - Q(f) s_W^2 \right], \\ a_f(Z_L) &= \frac{e}{s_W c_W} \frac{T_{3L}(f_L)}{2}, \\ v_f(Z_R) &= -\frac{e}{2s_W \sqrt{x^2 + y^2}} \left\{ y^2 [\tilde{Y}(f_L) + \tilde{Y}(f_R)] \right\}, \\ a_f(Z_R) &= -\frac{e}{2s_W \sqrt{x^2 + y^2}} \left\{ y^2 [\tilde{Y}(f_L) - \tilde{Y}(f_R)] \right\}. \end{aligned} \quad (\text{B.4})$$

$$v_f(Z') = -s_0 v_f(Z_L) + c_0 v_f(Z_R), \quad a_f(Z') = -s_0 v_f(Z_L) + c_0 v_f(Z_R). \quad (\text{B.5})$$

The Z' partial decay rates into fermion pairs are then given by the standard formulae:

$$\Gamma(Z' \rightarrow f \bar{f}) = \frac{m_{Z'}}{12\pi} (1 - 4\eta'_f)^{1/2} C_f \left\{ v_f^2(Z') + a_f^2(Z') + 2[v_f^2(Z') - 2a_f^2(Z')] \eta'_f \right\}, \quad (\text{B.6})$$

where $C_f = 1, 3$ is the colour factor and $\eta'_f \equiv m_f^2/m_{Z'}^2$.

From the explicit expressions of the trilinear gauge boson vertices, given in appendix A, we can easily derive the Z' and W' decay rates into gauge bosons, when the processes are kinematically allowed:

$$\Gamma(Z' \rightarrow W^+ W^-) = \frac{m_{Z'}}{192\pi} \eta_{WZ'}^{-2} (1 - 4\eta_{WZ'})^{3/2} (1 + 20\eta_{WZ'} + 12\eta_{WZ'}^2) \delta^2(Z' W W), \quad (\text{B.7})$$

where $\eta_{WZ'} \equiv m_W^2/m_{Z'}^2$ and

$$\delta(Z' W W) = g \left(c_W s_0 c_\pm^2 - \frac{x}{y} t_W c_0 s_\pm^2 - s_W t_W s_0 s_\pm^2 \right). \quad (\text{B.8})$$

$$\Gamma(Z' \rightarrow W W') = \frac{m_{Z'}}{192\pi} \eta_{WZ'}^{-1} \eta_{W'Z'}^{-1} \left[(1 - \eta_{WZ'} + \eta_{W'Z'})^2 - 4\eta_{W'Z'} \right]^{3/2} \quad (\text{B.9})$$

$$\left[1 + 10(\eta_{W'Z'} + \eta_{WZ'}) + \eta_{W'Z'}^2 + \eta_{WZ'}^2 + 10\eta_{W'Z'}\eta_{WZ'}\right] \delta^2(Z'WW'), \quad (\text{B.10})$$

where $\eta_{W'Z'} \equiv m_{W'}^2/m_{Z'}^2$, $\eta_{WZ'} \equiv m_W^2/m_{Z'}^2$, and

$$\delta(Z'WW') = gs_{\pm}c_{\pm} \left(\frac{s_0}{c_W} + \frac{x}{y}t_Wc_0 \right). \quad (\text{B.11})$$

$$\Gamma(Z' \rightarrow W'W') = \frac{m_{Z'}}{192\pi} \eta_{W'Z'}^{-2} (1 - 4\eta_{W'Z'})^{3/2} (1 + 20\eta_{W'Z'} + 12\eta_{W'Z'}^2) \delta^2(Z'W'W'), \quad (\text{B.12})$$

where $\eta_{W'Z'} \equiv m_{W'}^2/m_{Z'}^2$, and

$$\delta(Z'W'W') = g \left(-c_W s_0 s_{\pm}^2 + \frac{x}{y} t_W c_0 c_{\pm}^2 + s_W t_W s_0 c_{\pm}^2 \right). \quad (\text{B.13})$$

$$\Gamma(W' \rightarrow WZ) = \frac{m_{W'}}{192\pi} \eta_{ZW'}^{-1} \eta_{WW'}^{-1} \left[(1 - \eta_{ZW'} + \eta_{WW'})^2 - 4\eta_{WW'} \right]^{3/2} \quad (\text{B.14})$$

$$\left[1 + 10(\eta_{WW'} + \eta_{ZW'}) + \eta_{WW'}^2 + \eta_{ZW'}^2 + 10\eta_{WW'}\eta_{ZW'} \right] \delta^2(W'WZ), \quad (\text{B.15})$$

where $\eta_{WW'} \equiv m_W^2/m_{W'}^2$, $\eta_{ZW'} \equiv m_Z^2/m_{W'}^2$, and

$$\delta(W'WZ) = gc_{\pm}s_{\pm} \left(\frac{c_0}{c_W} - s_0 \frac{x}{y} t_W \right). \quad (\text{B.16})$$

From the explicit expressions of the cubic bosonic couplings involving the SM-like Higgs h and pairs of vector bosons, given in appendix A, we can easily derive the Z' and W' decay rates into final states involving gauge and Higgs bosons, when the processes are kinematically allowed:

$$\Gamma(Z' \rightarrow Zh) = \frac{m_{Z'}}{192\pi} \left[(1 - \eta_{hZ'} + \eta_{ZZ'})^2 - 4\eta_{ZZ'} \right]^{1/2} \quad (\text{B.17})$$

$$\left[1 + \eta_{hZ'}^2 + \eta_{ZZ'}^2 + 10\eta_{ZZ'} - 2\eta_{hZ'} - 2\eta_{hZ'}\eta_{ZZ'} \right] \left[\frac{\delta(Z'Zh)}{m_Z} \right]^2, \quad (\text{B.18})$$

$$\Gamma(W' \rightarrow Wh) = \frac{m_{W'}}{192\pi} \left[(1 - \eta_{hW'} + \eta_{WW'})^2 - 4\eta_{WW'} \right]^{1/2} \quad (\text{B.19})$$

$$\left[1 + \eta_{hW'}^2 + \eta_{WW'}^2 + 10\eta_{WW'} - 2\eta_{hW'} - 2\eta_{hW'}\eta_{WW'} \right] \left[\frac{\delta(W'Wh)}{m_W} \right]^2, \quad (\text{B.20})$$

where $\eta_{hZ'} \equiv m_h^2/m_{Z'}^2$, $\eta_{hW'} \equiv m_h^2/m_{W'}^2$, and

$$\delta(Z'Zh) = \frac{(g_R^2 + \tilde{g}^2)v_R^2}{2\sqrt{v_L^2 + v_1^2 + v_2^2}} s_0 c_0, \quad (\text{B.21})$$

$$\delta(W'Wh) = \frac{g_R^2 v_R^2}{2\sqrt{v_L^2 + v_1^2 + v_2^2}} s_{\pm} c_{\pm}. \quad (\text{B.22})$$

It is important to notice the following asymptotic relations, valid when $m_{W',Z'} \gg m_{W,Z}$:

$$\delta^2(Z'WW) \rightarrow g^2 c_W^2 s_0^2, \quad \delta^2(W'WZ) \rightarrow \frac{g^2 s_\pm^2}{c_W^2}, \quad (\text{B.23})$$

$$\delta^2(Z'Zh) \rightarrow \frac{g^2 s_0^2 m_{Z'}^4}{m_W^2}, \quad \delta^2(W'Wh) \rightarrow \frac{g^2 s_\pm^2 m_{W'}^4}{m_W^2}, \quad (\text{B.24})$$

$$\frac{\Gamma(Z' \rightarrow WW)}{\Gamma(Z' \rightarrow Zh)} \rightarrow 1, \quad \frac{\Gamma(W' \rightarrow WZ)}{\Gamma(W' \rightarrow Wh)} \rightarrow 1. \quad (\text{B.25})$$

For convenience, we rewrite the expressions for the triple bosonic couplings at the lowest order in α_\pm, α_0 :

$$\delta(Z'WW) = g c_W \alpha_0, \quad \delta(W'WZ) = \frac{g}{c_W} \alpha_\pm, \quad (\text{B.26})$$

$$\delta(Z'WW') = g \frac{x}{y} t_W \alpha_\pm, \quad \delta(Z'W'W') = g \frac{x}{y} t_W, \quad (\text{B.27})$$

$$\delta(Z'Zh) = \frac{(g_R^2 + \tilde{g}^2) v_R^2}{2\sqrt{v_L^2 + v_1^2 + v_2^2}} \alpha_0, \quad \delta(W'Wh) = \frac{g_R^2 v_R^2}{2\sqrt{v_L^2 + v_1^2 + v_2^2}} \alpha_\pm. \quad (\text{B.28})$$

References

- [1] J.C. Pati and A. Salam, Phys. Rev. D10 (1974) 275;
R.N. Mohapatra and J.C. Pati, Phys. Rev. D11 (1975) 566 and 2558;
G. Senjanovic and R.N. Mohapatra, Phys. Rev. D12 (1975) 1502.
- [2] R.N. Mohapatra and R.E. Marshak, Phys. Lett. B91 (1980) 222;
D. Cocolicchio and G.L. Fogli, Phys. Rev. D32 (1985) 3020;
N.G. Deshpande, J.A. Grifols and A. Mendez, Phys. Lett. B208 (1988) 141, Erratum-
ibid. B214 (1988) 661;
J.F. Gunion, J. Grifols, A. Mendez, B. Kayser and F. Olness, Phys. Rev. D40 (1989)
1546;
F. Feruglio, L. Maiani and A. Masiero, Phys. Lett. B233 (1989) 512;
J. Polak and M. Zralek, Nucl. Phys. B363 (1991) 385, Phys. Rev. D46 (1992) 387 and
Phys. Lett. B276 (1992) 492;
A. Deandrea, F. Feruglio and G.L. Fogli, Nucl. Phys. B402 (1993) 3;
O.M. Boyarkin, Phys. Rev. D50 (1994) 2247;
A. Pilaftsis, Phys. Rev. D52 (1995) 459.
- [3] V. Barger, W.Y. Keung and E. Ma, Phys. Rev. D22 (1980) 727 and Phys. Lett. B94
(1980) 377;
V. Barger, E. Ma and K. Whisnant, Phys. Rev. Lett. 46 (1981) 1501;
J.L. Kneur and D. Schildknecht, Nucl. Phys. B357 (1991) 357.
- [4] H. Georgi, E.E. Jenkins and E.H. Simmons, Phys. Rev. Lett. 62 (1989) 2789 +(E) 63
(1989) 1540 and Nucl. Phys. B331 (1990) 541;
E. Ma and S. Rajpoot, Mod. Phys. Lett. A5 (1990) 979;
V. Barger and T. Rizzo, Phys. Rev. D41 (1990) 946;
L. Randall, Phys. Lett. B234 (1990) 508;
T.G. Rizzo, Int. Jour. Mod. Phys. A7 (1992) 91;
R.S. Chivukula, E.H. Simmons and J. Terning, Phys. Lett. B346 (1995) 284.
- [5] D.J. Muller and S. Nandi, Phys. Lett. B383 (1996) 345;
E. Malkawi, T. Tait and C.-P. Yuan, Phys. Lett. B385 (1996) 304.
- [6] M. Bilenky, J.-L. Kneur, F.M. Renard and D. Schildknecht, Phys. Lett. B316 (1993)
345;
R. Casalbuoni, A. Deandrea, S. De Curtis, D. Dominici, R. Gatto and M. Grazzini,
Phys. Rev. D53 (1996) 5201;
R. Casalbuoni, P. Chiappetta, A. Deandrea, S. De Curtis, D. Dominici and R. Gatto,
hep-ph/9702325;
R. Casalbuoni, S. De Curtis and D. Dominici, hep-ph/9702357.

- [7] Particle Data Group, Phys. Rev. D54 (1996) 1;
The LEP Electroweak Working Group, preprint CERN-PPE/96-183 and Internal Note LEPEWWG 97-01;
C.S. Wood et al., Science 275 (1997) 1759.
- [8] G. Altarelli, R. Casalbuoni, D. Dominici, F. Feruglio and R. Gatto, Nucl. Phys. B342 (1990) 15;
G. Altarelli, N. Di Bartolomeo, F. Feruglio, R. Gatto and M.L. Mangano, Phys. Lett. B375 (1996) 292.
- [9] J. Matias and A. Vicini, in preparation.
- [10] P. Sikivie, L. Susskind, M. Voloshin and V. Zakharov, Nucl. Phys. B173 (1980) 189;
D. Toussaint, Phys. Rev. D18 (1978) 1626;
M.B. Einhorn and J. Wudka, Phys. Rev. D47 (1993) 5029.
- [11] R. Casalbuoni, S. De Curtis, D. Dominici and R. Gatto, Phys. Lett. B155 (1985) 95 and Nucl. Phys. B282 (1987) 235.
- [12] A. Djouadi, J.L. Kneur and G. Moultaka, Phys. Lett. B242 (1990) 265;
W. Hollik, Mod. Phys. Lett. A5 (1990) 1909.
- [13] A. Brignole, F. Feruglio and F. Zwirner, Z. Phys. C71 (1996) 679.
- [14] G. Beall, M. Bander and A. Soni, Phys. Rev. Lett. 48 (1982) 848;
G. Ecker and W. Grimus, Nucl. Phys. B258 (1985) 328;
P. Langacker and S. Uma Sankar, Phys. Rev. D40 (1989) 1569;
J. M. Frere, J. Galand, A. Le Yaouanc, L. Oliver, O Pene and J.C. Raynald, Phys. Rev. D46 (1992) 337;
P. Cho and M. Misiak, Phys. Rev. D49 (1994) 5894;
M. E. Pospelov, hep-ph/9611422.
- [15] G. Isidori, Phys. Lett. B298 (1993) 409;
Y. Grossman and Z. Ligeti, Phys. Lett. B332 (1994) 373;
A. Stahl and H. Voss, Z. Phys. C74 (1997) 73;
J.A. Coarasa, R.A. Jiménez and J. Solà, hep-ph/9701392.
- [16] F. Abe et al. (CDF Collaboration), preprint FERMILAB-PUB-97/058-E.
- [17] M.S. Alam et al. (CLEO Collaboration), Phys. Rev. Lett. 71 (1993) 674 and 74 (1995) 2885.
- [18] K. Chetyrkin, M. Misiak and M. Münz, preprint hep-ph/9612313;
C. Greub, T. Hurth and D. Wyler, Phys. Lett. B380 (1996) 385 and Phys. Rev. D54 (1996) 3350;

- K. Adel and Y.P. Yao, Phys. Rev. D49 (1994) 4945;
A. Ali and C. Greub, Phys. Lett. B361 (1995) 146.
- [19] C. Q. Geng and J. N. Ng, Phys. Rev. D38 (1988) 2857;
W.-S. Hou and R. S. Willey, Phys. Lett. B202 (1988) 591;
T. Rizzo, Phys. Rev. D38 (1988) 820;
X.-G. He, T. D. Nguyen and R. R. Volkas, Phys. Rev. D38 (1988) 814;
M. Ciuchini, Mod. Phys. Lett. A4 (1989) 1945.
- [20] A. Buras, P. Krawczyk, M. Lautenbacher and C. Salazar, Nucl. Phys. B337 (1990) 284 and references therein.
- [21] M. Crisafulli, A. Donini, V. Lubicz, G. Martinelli, F. Rapuano, M. Talevi, C. Ungarelli and A. Vladikas, Phys. Lett. B369 (1996) 325;
A. Donini, V. Gimenez, G. Martinelli, M. Talevi and A. Vladikas, in preparation.
- [22] J. Botts, J.G. Morfin, J.F. Owens, J. Qiu, W.K. Tung and H. Weerts, Phys. Lett. B304 (1993) 159.
- [23] F. Abe et al., The CDF Collaboration, FERMILAB-PUB-97/122-E;
C.E. Gerber, for the D0 Collaboration, in the Proceedings of the Division of Particles and Fields meeting, Minneapolis/St. Paul, Minnesota 1996, FERMILAB-CONF-96/389-E.
- [24] I.A Bertram, for the D0 Collaboration, in the Proceedings of the Division of Particles and Fields meeting, Minneapolis/St. Paul, Minnesota 1996, FERMILAB-CONF-96/389-E;
F. Abe et al., The CDF Collaboration, FERMILAB-PUB-97/023-E.
- [25] D. Benjamin, in Proceedings of the *XXXIst* Rencontres de Moriond, "'96 Electroweak Interactions and Unified Theories", Les Arcs, Savoie, France 1996, Ed. Frontieres, 96 France, pp. 103-110.
- [26] F. del Aguila, M. Quirós and F. Zwirner, Nucl. Phys. B284 (1987) 530 and B287 (1987) 419.